1966

Noise in thin magnetic film parametric amplifiers from 78° K to 300° K

Charles Teh-chuan Chen
Iowa State University

CHEN, Charles Teh-chuan, 1935-

NOISE IN THIN MAGNETIC FILM PARAMETRIC AMPLIFIERS FROM 78°K TO 300°K.

Iowa State University of Science and Technology, Ph.D., 1966
Engineering, electrical

University Microfilms, Inc., Ann Arbor, Michigan

NOISE IN THIN MAGNETIC FILM PARAMETRIC AMPLIFIERS FROM 78°K TO 300°K

by

Charles Teh-chuan Chen

A Dissertation Submitted to the

Graduate Faculty in Partial Fulfillment of

The Requirements for the Degree of

DOCTOR OF PHILOSOPHY

Major Subject: Electrical Engineering

Approved:

Signature was redacted for privacy.

In Charge of Major Work

Signature was redacted for privacy.

Head of Major Department

Signature was redacted for privacy.

Dean of Graduate College

Iowa State University
Of Science and Technology
Ames, Iowa
1966

TABLE OF CONTENTS

I. INTRODUCTION

The purpose of this thesis was to evaluate and analyze the noise performance of thin magnetic films in a parametric amplifier operating over an extended temperature ($78^{o}K$ to $300^{o}K$).

More specifically, the objectives of this research were to determine the following:

A. What sort of noise performance do magnetic film parametric amplifiers have when operated over an extended temperature range?

B. Can improved performance be obtained by cooling the elements of the amplifier?

C. What factors contribute to the noise performance of thin magnetic film parametric amplifiers?

D. What improvements can be made over present devices?

To achieve the stated objectives a few thin magnetic film parametric amplifiers were constructed and a number of experiments were performed. The experiments and the results are discussed in the body of this thesis.

II. REVIEW OF PERTINENT LITERATURE AND PAST DEVELOPMENTS

A parametric amplifier is a device with an energy storage element(s) whose value(s) can be made to vary in a proper way. When an energy storage element(s) is (are) suitably coupled to one or more resonant circuit(s), energy may be extracted from the source which drives the energy storage element and transfers it to the resonant circuit. Therefore a signal can be amplified.

In 1936 R. V. L. Hartley (1) discussed in great detail an electro-mechanical nonlinear capacitance device very similar to today's negative resistance parametric amplifier. In 1948 Van der Ziel, A. (2) analyzed a circuit containing nonlinear capacitance and also first mentioned that such a circuit might have a very low noise factor.

Three types of parametric amplifiers were considered by Rowe (3):

A. Noninverting modulator or demodulator-signal frequencies are f_1 and f_2, and $f_2 = f_1 + f_p$, where f_p is the pumping frequency. This device is stable and its maximum gain is equal to the ratio of output to input frequency as predicted by Manley - Rowe Power equations (4). The typical device is a parametric upconverter.

B. Inverting modulator and demodulator-signal frequencies are f_1 and f_2, and $f_2 = f_p - f_1$. This device is potentially unstable. The transducer gain can take on any value between zero and infinity, depending on the external impedances at the signal terminals. For a larger amount of nonlinearity, substantially

greater gains can be obtained with moderate bandwidth and sensitivity. The typical device is the lower sideband converter.

C. Negative resistance parametric amplifier-this is the one special case of type B with the same input and output frequency. Substantial gain at the moderate bandwidth and sensitivity may be obtained, as with the lower sideband converter. For a given nonlinearity, high gain implies a narrow bandwidth since the gain bandwidth product is constant. If the bandwidth of the input and output frequency overlaps, the parametric amplifier is called a degenerative parametric amplifier, otherwise a nondegenerative parametric amplifier. In this thesis a nondegenerative parametric amplifier was used for the noise measurement. Therefore its noise performance is of a special interest to us. If the losses of a parametric element can be negligible for an ideal nonlinear reactance, the minimum noise figure obtainable from this parametric amplifier is:

$$F = 1 + \frac{T_2}{T_g} \frac{\omega_1}{\omega_2}$$

where ω_1 and ω_2 are angular frequencies of signal and idler respectively, and T_2 and T_g are temperatures of idler and input termination. This equation shows the noise figure of an amplifier can be reduced by decreasing the signal to idler frequency ratio or by cooling the idler tank. Neither the thin film inductor nor the back-biased diode are lossless.

The loss of a parametric element will contribute the thermal noise to the amplifier and also reduce the conversion efficiency. Therefore the quality factor of a parametric element was used to characterize the operation of a parametric amplifier (5), (6).

In 1959 Read and Pohm (7) successfully developed magnetic film parametric amplifiers; Pohm, Read, Stewart and Schauer (8) also proposed the magnetic film parametrons for computer logic. The noise characteristics of thin ferromagnetic film devices were investigated by Samuels (9) before. He observed: (a) the noise performance of thin magnetic film parametric amplifiers were improved by increasing the bias current; (b) the noise figure was increased by heating the magnetic film; and (c) while cooling the parametric elements, some parametric amplifiers show decreases in noise figure and some, however, show increases. It indicates that films are subject to strain during cooling.

The noise figure of a parametric amplifier is a function of circuit parameters, temperature of circuit elements and the frequency ratio of signal and idler. Kurokawa and Uenohala (10) have plotted minimum noise figure of parametric amplifier vs. dynamic quality factor of the parametric element with signal to idler frequency ratio as a parameter. It is very advantageous to keep signal to idler frequency ratio low to obtain a wider constant noise figure region, although the minimum noise figure of an amplifier is higher because the quality factor of a parametric element depends on the bias.

The Barkhausen effect is usually ascribed to the following mechanism: In a ferromagnetic material with a small increase in magnetic field, the

boundary between domains is displaced such that those domains magnetized with components parallel to the field expand, absorbing those less favorably magnetized to keep the minimum sum of all the magnetic energies. At first a given boundary will move reversibly, until a boundary meets an obstacle on its path; (stress irregularities, non-ferromagnetic inclusions, etc.). Then it may be delayed by them. The delay mechanism was explained by Rodichev and Ignatchenko (11) by means of Figure (1). Suppose P in Figure (1) is the position of obstacle. When the boundary reaches P, it will stand fixed, (more precisely, it will slowly shift without breaking away from the obstacle) until the external field overcomes the additional magnetostatic energies due to the presence of obstacle; the boundary will then jump away from the obstacle. It follows that the boundary may make two jumps on one obstacle: one on approaching close to the inclusion and one on tearing away from it. It was suggested by Tebble and Newhouse (12) that the Barkhausen effect is to be associated with the movement of 180° rather than 90° boundary. They also mentioned that the effect of a high demagnetizing factor is to reduce the magnitude of the Barkhausen effect and to produce a corresponding increase in the contribution of the reversible magnetization processes. Recently, Salanskiy and Rocichev (13) investigated the length distribution of Barkhausen pulses and found different characteristics for massive cylindrical specimens and thin films. They concluded: "In films the length of the Barkhausen pulse should be substantially dependent on the nature of the sudden change in the intensity of magnetization." In their experimental result, the average length of a Barkhausen pulse was 4.8 μ sec in the easy direction and 1.95 μ sec in the hard direction. They

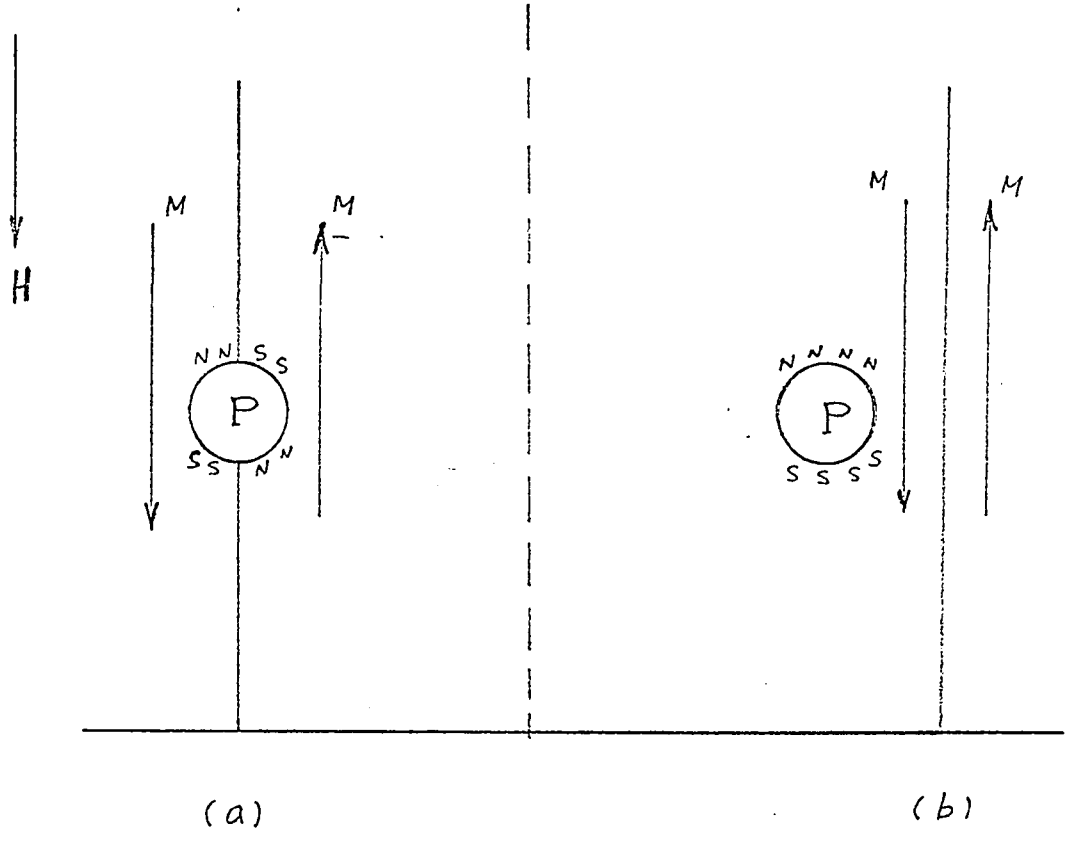

Figure 1. The delay mechanism in a non-ferromagnetic inclusion
a) Boundary delayed on an inclusion shown by the distribution of poles
b) Boundary tears away from obstacle as a result of the increase in the magnetostatic energy

suggested that differences are due to two different jump mechanicms: "When remagnetization occurs in the easy direction the jump means a shift of the 180^{o} boundary while in the difficult direction the magnetic moment probably rotates through 90^{o}. In the later case there should be a considerable increase in the rate of process."

The length of Barkhausen impulses determines the frequency characteristics of the noise spectra during cyclic magnetization. Krumhansl and Beyer (14) consider the noise produced by the random superposition of many elementary pulses and find the Barkhausen noise is proportional to the frequency of the magnetizing field. The frequency spectrum of the Barkhausen noise was also theoretically and experimentally investigated by Biorci and Pescetti (15). The computed spectral density is constant up to 1 kcps and then decreases exponentially. The frequency of magnetizing field used in their experiment was 1.5 cps.

As to the temperature effect of the Barkhausen discontinuities, Stierstadt and Pfrenger (16) used nickel samples of different purity and of different thermal treatment and investigated in the temperature range from liquid air up to the curie point. They concluded: (a) the size distribution of two samples, having in practice the same hysterisis loop can show a completely different behavior as a function of the magnetic field; (b) the number of great discontinuities is reduced more rapidly with the rising temperature than that of the smaller ones; (c) the Barkhausen part of the total magnetization varies with temperature like the coercive force and therefore seems to be a structure-dependent quantity.

The effect of Barkhausen jumps at different elastic stresses were

investigated by Kirenskiy, Salanskiy and Rodichev (17). Their results are: (a) The number of Barkhausen jumps increased considerably with the increasing stress. (b) The length of the actual jump becomes greater with the rising stress, i.e. the domain boundary in a jump extends to a much greater distance.

From the comparison with pertinent literature on the Barkhausen effect, the following conclusions are obtained:

A. Two samples with the same hysteresis loop may show completely different behavior in their Barkhausen noise. The size distribution of the Barkhausen pulses of two samples with the same hysteresis loop can show a completely different behavior as a function of the magnetic field (16).

B. The length distribution of Barkhausen pulses indicates that the durations of pulses decrease with increasing field intensity (13). The Barkhausen noise should increase accordingly if the number of jumps is the same.

C. The number of Barkhausen jumps increases considerably with the increasing stress and the length of actual jump becomes greater with rising stress (17). These might indicate the motion of magnetization would slow down and the Barkhausen noise might be higher when magnetic material is being stressed. This conclusion would apply in our low temperature experiment.

III. A THIN FILM TIME VARYING INDUCTOR

The equation of motion and damping of magnetization when subjected to time varying external magnetic field was proposed by Landau and Lifshitz (18). This can be linearized and applied to magnetic films for small oscillations of the magnetization. The equation in rationalized MKS system is (19):

$$\frac{\mu_o}{\gamma_1^2 M}\ddot{\Phi} + \frac{\lambda}{\gamma_1^2 M}\dot{\Phi} + (H_k + H_x)\,\Phi = H_y \qquad (1)$$

where μ_o = permeability of free space = $4\pi \times 10^{-7}$ henries per meter

$\gamma_1 = \frac{g\mu_o e}{2m} = 2.30 \times 10^5$ radians per second per ampere-turn per meter

M = magnitude of saturated magnetization in weber per meter square

H_k = anisotropy field in ampere-turn per meter

H_x = applied external field in easy direction in ampere-turn per meter

H_y = applied external field in hard direction in ampere-turn per meter

λ = damping constant = 10^{-8} cps

Φ = angle of rotation of magnetization in the plane of film in radians $\dot{\Phi} = \frac{d\Phi}{dt}$ and $\ddot{\Phi} = \frac{d^2\Phi}{dt^2}$

The flux density within the material can be written as

$$\underline{B} = \mu_o \underline{H} + \underline{M}, \qquad (2)$$

and for the y component $B_y = \mu_o H_y + M\sin\Phi$. (3)

The total flux linkage in the hard direction then is obtained by multiplying the cross sectional area in hard direction of the material A_m by the flux density B_y.

$$\lambda_y(t) = \mu_o A_m H_y + A_m M \sin\Phi$$

$$\text{where } \lambda_y = A_m B_y \tag{4}$$

The voltage (e_y) induced on the coil whose axis is in the hard direction of film can be represented by:

$$e_y = \frac{d\lambda_y}{dt} \cong \lambda_{mt} \dot{\Phi} \tag{5}$$

assuming $\mu_o A_m H_y << A_m M \sin\Phi$, $A_m M = \lambda_{mt}$ and $\sin\Phi \cong \Phi$.

Substituting Equation (5) into Equation (1) and using the relation $H_y = \frac{N_s I_s}{r}$, where N_s and r are number of turns and length of coil as shown in Figure 2 it yields:

$$\frac{\mu_o r}{\gamma_1^2 M \lambda_{mt} N_s} \dot{e}_y + \frac{\lambda r}{\gamma_1^2 M \lambda_{mt} N_s} e_y + \frac{(H_k + H_x) r}{\lambda_{mt} N_s} \int e_y \, dt = i_y \tag{6}$$

or

$$C_o \dot{e}_y + \frac{1}{R_o} e_y + \frac{1}{L_o} \int e_y \, dt = i_y \tag{7}$$

where

$$C_o = \frac{\mu_o r}{\gamma_1^2 M \lambda_{mt} N_s}$$

$$R_o = \frac{\gamma_1^2 M \lambda_{mt} N_s}{\lambda_r}$$

$$L_o = \frac{\lambda_{mt} N_s}{(H_k + H_x) r} \tag{8}$$

The resonant frequency of the system is

$$f_r = \frac{\gamma_1}{2\pi} \sqrt{\frac{M}{\mu_o} (H_k + H_x)} \tag{9}$$

For H_x =), the resonant frequency is estimated to be about 450 MC (19).

The equivalent circuit of thin film inductor is as shown in Figure 3. If a d.c. bias (H_B) and a time varying field ($H_p \cos\omega_p t$) are applied in the easy direction of the film and if both the loss term and the capacitive term are small and can be neglected, the inductance across the coil is given by:

$$L(t) = \frac{\lambda_{mt} N_s}{r(H_B + H_k + H_p \cos\omega_p t)}$$

$$= \frac{\lambda_{mt} N_s}{r(H_B + H_k)} \left(1 + \frac{H_p \cos\omega_p t}{H_B + H_k}\right)^{-1} \qquad (10a)$$

assuming $\frac{H_p}{H_B + H_k} < 1$.

If a power series expansion is made for the expression for L(t) and the higher order terms of $\frac{H_p}{H_B + H_k}$ are neglected, the time varying inductance can be expressed as:

$$L(t) = L_o' \left((1 + \tfrac{1}{2}p^2 + 3/8p^4) - (p + 3/4p^3) \cos\omega_p t \right.$$

$$\left. + (\tfrac{1}{2}p^2 + \tfrac{1}{2}p^4) \cos 2\omega_p t - \tfrac{1}{4}p^3 \cos 3\omega_p t + 1/8p^4 \cos 4\omega_p t + \ldots \right) \qquad (10b)$$

where $p = \frac{H_p}{H_B + H_k}$ and $L_o' = \frac{\lambda_{mt} N_s}{r(H_k + H_B)}$.

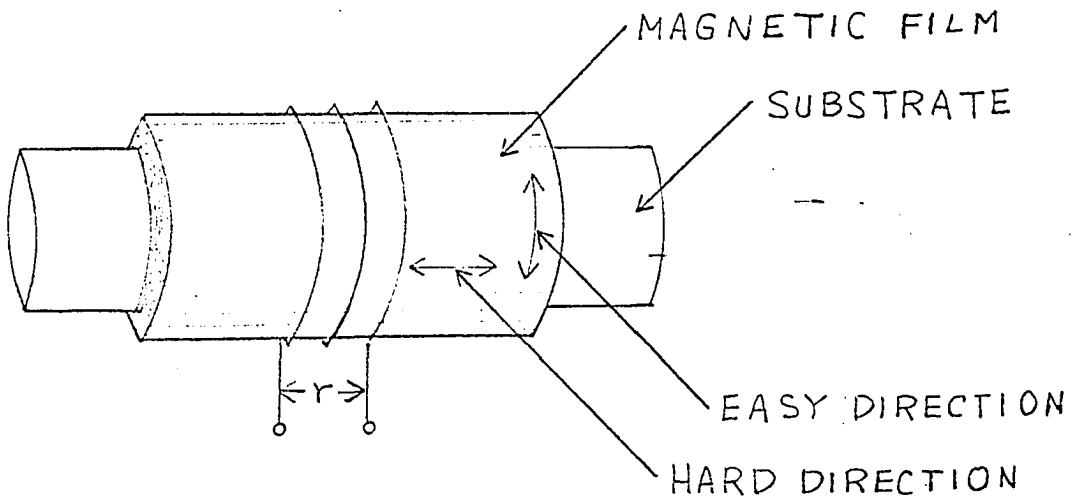

Figure 2. The schematic representation of the thin film parametric inductor

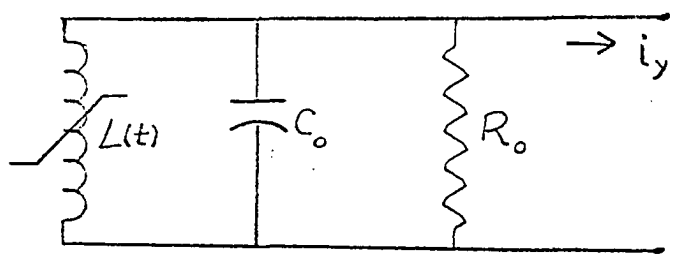

Figure 3. Idealized equivalent circuit of the thin film inductor

IV. PARAMETRIC AMPLIFIERS

A. A Thin Magnetic Film Inductor as a Parametric Element

In the analysis of parametric devices, we are interested in computing the mixing effects that occur when currents or voltages at two or more different frequencies are impressed on a nonlinear reactance. In this investigation, we have three frequencies--the pumping frequency (ω_p), the signal frequency (ω_1), and the idler frequency (ω_2). One quantity of interest is the resultant signal voltage for an assumed current at the signal frequency. One can obtain an equivalent linear impedance which the remainder of the circuit presents at ω_1. Once this impedance is determined, the power gain and bandwidth of the parametric devices can be obtained by linear analysis.

Assuming the circuit design is properly made such that only the signal current at frequency ω_1 and the idler current at frequency $\omega_p - \omega_1$ flows through the time varying inductance, it is convenient to evaluate the voltage at ω_1 and $\omega_p - \omega_1$ as a function of the currents, obtaining an equivalent linearized impedance matrix. The time varying inductance can then be replaced by this matrix whenever we wish to compute the characteristics of a parametric device.

To construct this impedance matrix, the inductance is treated in a complex form. From Equation (10b) and neglecting the harmonic terms, one obtains

$$L(t) = L_o - L_1 \cos\omega_p t = L_o - \tfrac{1}{2}L_1(e^{j\omega_p t} + e^{-j\omega_p t}) \qquad (11)$$

where $L_o = L_o' \, (1 + \tfrac{1}{2}p^2 + 3/8p^4)$

$L_1 = L_o' \, (p + 3/4p^3)$

In a similar manner, the current and the voltage across the thin film inductor are expressed as:

$$i = I_1 e^{j\omega_1 t} + I_1^* e^{-j\omega_1 t} + I_2 e^{j\omega_2 t} + I_2^* e^{-j\omega_2 t)} \tag{12}$$

$$v = V_1 e^{j\omega_1 t} + V_1^* e^{-j\omega_i t} + V_2 e^{j\omega_2 t} + V_2^* e^{-j\omega_2 t)} \tag{13}$$

where $\omega_1 + \omega_2 = \omega_p$. The asterisk means the complex conjugate. The coefficients I_1, I_2, V_1, V_2 are complex quantities containing the phase information. The current and the voltage are related by

$$V = - \frac{d}{dt} (Li) \tag{14}$$

Equations (11), (12) and (13) are substituted into Equation (14) and impedance matrix equation is obtained:

$$\begin{bmatrix} V_1 \\ V^*_2 \end{bmatrix} = \begin{bmatrix} -j\omega_1 L_o & j\omega_1 L_o \gamma \\ -j\omega_2 L_o \gamma & j\omega_2 L_o \end{bmatrix} \begin{bmatrix} I_1 \\ I^*_2 \end{bmatrix} \tag{15}$$

where $\gamma = \frac{L_1}{2L_o}$.

B. Circuit Model for the Inverting Type Parametric Amplifiers

The inverting type parametric amplifiers to be considered are the lower sideband frequency converter and the negative resistance parametric amplifier. The generalized circuit model for the inverting type parametric amplifiers can be represented as shown in Figure 4. The diagonal terms in the impedance matrix that do not contribute to the energy conversion are absorbed into Z_{11} or Z_{22}. R_{s1} and R_{s2} are loss resistances of parametric element at ω_1 and ω_2 respectively. The

simplified impedance matrix is accordingly:

$$\begin{bmatrix} V_1 \\ V^*_2 \end{bmatrix} = \begin{bmatrix} 0 & j\omega_1 L_o \gamma \\ -j\omega_2 L_o \gamma & 0 \end{bmatrix} \begin{bmatrix} I_1 \\ I^*_2 \end{bmatrix} \tag{16}$$

Let one define the dynamic quality factors (Q_1, Q_2) and static quality factor (Q_{10}, Q_{20}) of the parametric element as

$$Q_1 = \frac{\omega_1 L_o \gamma}{R_{s1}} \qquad Q_2 = \frac{\omega_2 L_o \gamma}{R_{s2}}$$

$$Q_{1o} = \frac{\omega_1 L_o}{R_{s1}} \qquad Q_{20} = \frac{\omega_2 L_o}{R_{s2}} \tag{17}$$

The loop equations of Figure 4 are

$$\begin{aligned} E_1 &= (Z_{11} + R_{s1}) I_1 + V_1 \\ &= (Z_{11} + R_{s1}) I_1 + j\omega_1 L_o \gamma I_2^* \\ &= (Z_{11} + R_{s1}) I_1 + jQ_1 R_{s1} I_2^* \end{aligned} \tag{18}$$

Similarly, one obtains

$$jQ_2 R_{s2} I_1^* + (Z_{22} + R_{s2}) I_2 = 0 \tag{19}$$

or

$$I_2^* = \frac{jQ_2 R_{s2} I_1}{Z_{22}^* + R_{s2}} \tag{20}$$

Substituting Equation (20) into Equation (18)

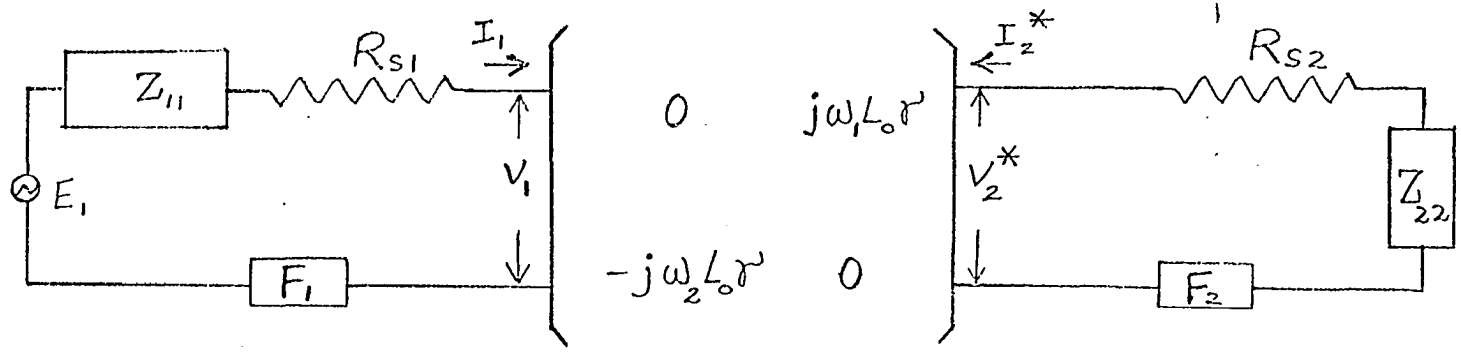

Figure 4. The circuit model for inverting type parametric devices. F_1 and F_2 are bandpass filter

$$I_1 = \frac{E_1}{Z_{11} + R_{s1}} - \frac{jQ_1R_{s1}}{Z_{11} + R_{s1}} I_2^*$$

$$= \frac{E_1}{Z_{11} + R_{s1}} + \frac{Q_1Q_2R_{s1}R_{s2}}{(Z_{22}^* + R_{s2})(Z_{11} + R_{s1})} I_1 \qquad (21)$$

or $$E_1 = (Z_{11} + R_{s1})\, I_1 - \frac{Q_1Q_2R_{s1}R_{s2}}{(Z_{22}^* + R_{s2})} I_1 \qquad (22)$$

When the complex conjugates of Equation (21) and substitute into Equation (19), the loop equation for the idler circuit is obtained.

$$- \frac{jQ_2R_{s2}}{Z_{11}^* + R_{s1}} E_1^* = (Z_{22} + R_{s2})I_2 - \frac{Q_1Q_2R_{s1}R_{s2}}{Z_{11}^* + R_{s1}} I_2 \qquad (23)$$

The linearized equivalent circuit for the signal and idler circuits as shown in Figure 5 are drawn from Equations (22) and (23). The characteristics of parametric devices therefore can be calculated from this linearized equivalent circuit.

C. The Lower Sideband Frequency Converter

This device with the input at frequency ω_1 and output at frequency of $\omega_p - \omega_1$ produces conversion gain because negative resistance is present across both the ω_1 circuit and the ω_2 circuit.

By inspection from Figure 5 the output power from the idler circuit is:

$$P_{21} = \frac{\left| \frac{Q_2R_{s2}E_1^*}{Z_{11}^* + R_{s1}} \right|^2 R_L}{\left| (R_{s2} + Z_{22}) - \frac{Q_1Q_2R_{s1}R_{s2}}{R_{s1} + Z_{11}^*} \right|^2} \qquad (24)$$

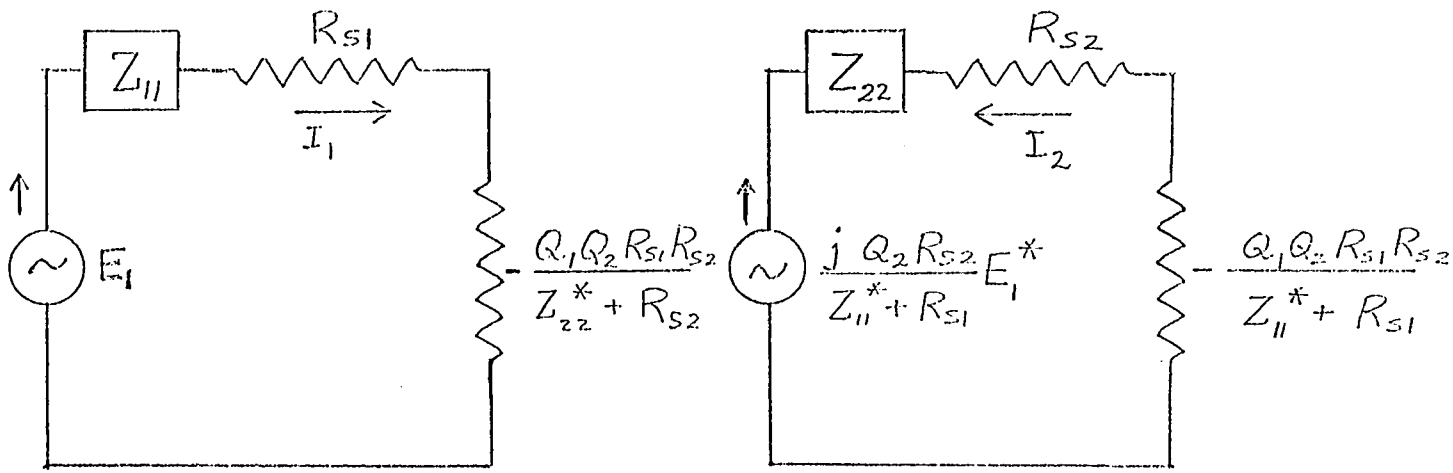

Figure 5. The linearized equivalent circuits for signal and idler circuits

where R_L is the load resistance and is considered as part of Z_{22}. The available input power is:

$$P_{av} = \frac{E_1^2}{4R_g} \tag{25}$$

where R_g is the internal resistance of signal generator. The conversion gain becomes:

$$G_{21} = \frac{P_{21}}{P_{av}} = \frac{4 R_g R_L \left| \frac{Q_2 Q_{s2}}{Z_{11}^* + R_{s1}} \right|^2}{\left| Z_{22} + R_{s2} - \frac{Q_1 Q_2 R_{s1} R_{s2}}{Z_{11}^* + R_{s1}} \right|^2}$$

$$= \frac{\frac{4R_g R_L}{R_{s1}^2} Q_2^2}{\left| (1 + \frac{Z_{22}}{R_{s2}})(1 + \frac{Z_{11}^*}{R_{s1}}) - Q_1 Q_2 \right|^2} \tag{26}$$

At the resonance:

$$G_{21} = \frac{\omega_2}{\omega_1} \frac{4R_g R_L \frac{R'}{R_{T1}}}{(R_{T2} - R')^2} \tag{27}$$

where $R' = \frac{\omega_1 \omega_2 L_o^2 Q^2}{R_{T1}}$

$$R_{T1} = R_{s1} + \mathrm{Re}(Z_{11}) = R_{s1} + R_1 + R_g$$

$$R_{T2} = R_{s2} + \mathrm{Re}(Z_{22}) = R_{s2} + R_2 + R_L$$

R_1 and R_2 are losses of tank circuits at ω_1 and ω_2 respectively.

To calculate the bandwidth, define:

Q_{T1} = the quality factor of tank 1, its resonant frequency is Ω_1

Q_{T2} = the quality factor of tank 2, its resonant frequency is Ω_2

Accordingly $\omega_1 = \Omega_1 + \Delta\omega$, $\Omega_1 + \Omega_2 = \omega_p$ and $\omega_2 = \Omega_2 - \Delta\omega$

The deviation away from the resonance can be expressed by the parameter which is defined as:

$$\delta = \frac{\Delta\omega}{\Omega_1}$$

Assuming series resonant circuits and employing the high -Q approximation, one can write the passive circuit impedances as:

$$Z_{11} + R_{s1} = R_{T1} (1 + j2\delta Q_{T1})$$

$$Z_{22} + R_{s2} = R_{T2} (1 - j2\delta Q_{T2} \frac{\Omega_1}{\Omega_2})$$

These relations are substituted into Equation (26). The conversion gain then can be expressed as:

$$G_{21} = \frac{4R_g R_L \left| \frac{\omega_2 L_o}{R_{T1}(1-j2\delta Q_{T1})} \right|^2}{\left| R_{T2} (1-j2\delta Q_{T2} \frac{\Omega_1}{\Omega_2}) - R' \right|^2}$$

$$= \frac{4 R_g R_L (\frac{\omega_2}{\omega_1}) (\frac{R'}{R_{T1}})}{(R_{T2} - R')^2 + 4\delta^2 ((R_{T2} - R') Q_{T1} + R_{T2} Q_{T2} \frac{\Omega_1}{\Omega_2})^2} \quad (28)$$

For 3 db fractional bandwidth, one sets the denominator of Equation (28) equal to twice that of Equation (26), or

$$2(R_{T2} - R')^2 = (R_{T2} - R')^2 + 4\delta^2 ((R_{T2} - R')Q_{T1} + R_{T2} Q_{T2} \frac{\Omega_1}{\Omega_2})^2$$

The 3 db fractional bandwidth becomes:

$$2\delta = \frac{R_{T2} - R'}{(R_{T2} - R')\, Q_{T1} + R_{T2}\, Q_{T2}\, \frac{\Omega_1}{\Omega_2}} \tag{29}$$

The gain bandwidth product of device is defined as

$$(\text{power gain})^{\frac{1}{2}}\ (\text{fractional bandwidth})$$

$$= \frac{2\,(R_g R_L \Omega_2 R'/\Omega_1 R_{T1})^{\frac{1}{2}}}{(R_{T2} - R')\, Q_{T1} + R_{T2}\, Q_{T2}\, \frac{\Omega_1}{\Omega_2}}$$

$$\cong 2\,\frac{1}{Q_{T2}}\,\left(\frac{\Omega_2}{\Omega_1}\right)^{3/2}\,\left(\frac{R_g R_L R'}{R_{T1} R_{T2}}\right)^{\frac{1}{2}} \tag{30}$$

where $R_{T2} Q_{T2} \frac{\Omega_1}{\Omega_2} >> (R_{T2} - R')\, Q_{T1}$ is assumed.

The noise figure of a parametric amplifier arises from the noise voltage in the ω_1 circuit as well as the noise voltage in the ω_2 circuit. Thermal noise explained in Appendix will be considered the predominant noise source. Although the dispersion of magnetic film and the thermal agitation of the magnetization contribute slightly to the noise, they will be considered part of the thermal noise.

The thermal noise voltage in the ω_1 circuit is given by:

$$e_{n1}^2 = 4kB(T_g R_g + T_1 R_1 + T_s R_{s1}) \tag{31}$$

The noise output power due to noise voltage in ω_1 circuit:

$$N_{21} = \frac{4kB\ (T_g R_g + T_1 R_1 + T_s R_{s1})\ (R_L / R_{s1}^2)\ Q_2^2}{\left| (1 + \frac{Z_{11}^*}{R_{s1}})\ (1 + \frac{Z_{22}}{\ }) - Q_1 Q_2 \right|^2} \tag{32}$$

Similarly the noise voltage in the ω_2 circuit is given by:

$$e_{n2}^2 = 4kB\ (T_2 R_2 + T_s R_{s2}) \tag{33}$$

The noise output power due to noise voltage in ω_2 circuit is:

$$N_{22} = \frac{4kB\ (T_2 R_2 + T_s R_{s2})\ R_L}{\left| (R_{s2} + Z_{22}) - \frac{Q_1 Q_2 R_{s1} R_{s2}}{R_{s1} + Z_{11}^*} \right|^2}$$

$$= \frac{4kB\ (T_2 R_2 + T_s R_{s2})\ (R_L / R_{s2}^2) \left| 1 + \frac{Z_{11}^*}{R_{s1}} \right|^2}{\left| (1 + \frac{Z_{11}^*}{R_{s1}})\ (1 + \frac{Z_{22}}{R_{s1}}) - Q_1 Q_2 \right|^2} \tag{34}$$

The noise factor of an amplifier has been defined in Appendix. Accordingly the noise factor of the converter is computed to be:

$$F_2 = \frac{N_{21} + N_{22}}{G_{s1} k T_g B} = 1 + \frac{T_1 R_1 + T_s R_{s1}}{T_g R_g}$$

$$+ \frac{T_2 R_2 + T_s R_{s2}}{T_g R_g} \quad \frac{\left| 1 + \frac{Z_{11}^*}{R_{s1}} \right|^2}{Q_2^2} \left(\frac{R_{s1}}{R_{s2}} \right)^2 \tag{35}$$

at resonance $Z_{11} = R_g + R_1$

and F_2 becomes

$$F_2 = 1 + \frac{T_1 R_1 + T_s R_{s1}}{T_g R_g} + \frac{T_2 R_2 + T_s R_{s2}}{T_g R_g} \quad \frac{(R_{s1} + R_1 + R_g)^2}{R' R_{s1}} \left(\frac{\omega_1}{\omega_2} \right) \tag{36}$$

where $-R' = -\dfrac{\omega_1 \omega_2 \gamma^2 L_o^2}{R_{s1}}$

D. Negative Resistance Parametric Amplifier

The analysis of this amplifier is quite similar to the lower sideband frequency converter. In this amplifier device output is extracted from the ω_1 circuit; therefore, the load resistance R_L is part of Z_{11} instead of Z_{22} as in the frequency converter.

By inspection from Figure 5, the power output is:

$$P_{11} = \frac{E_1^2 R_L}{\left|(R_{s1} + Z_{11}) - \dfrac{Q_1 Q_2 R_{s1} R_{s2}}{R_{s2} + Z_{22}^*}\right|^2}$$

$$= \frac{(E_1)^2 \dfrac{R_L}{R_{s1}^2} \left|1 + \dfrac{Z_{22}^*}{R_{s2}}\right|^2}{\left|(1 + \dfrac{Z_{11}}{R_{s1}})(1 + \dfrac{Z_{22}^*}{R_{s2}}) - Q_1 Q_2\right|^2} \qquad (37)$$

and the power gain is:

$$G_{11} = \frac{P_{11}}{\dfrac{(E_1)^2}{4R_g}} = \frac{\dfrac{4R_L R_g}{R_{s1}^2} \left|1 + \dfrac{Z_{22}^*}{R_{s1}}\right|^2}{\left|(1 + \dfrac{Z_{11}}{R_{s1}})(1 + \dfrac{Z_{22}^*}{R_{s2}}) - Q_1 Q_2\right|^2} \qquad (38)$$

At resonance $R_{s2} + Z_{22} = R_{s2} + R_2 = R_{T2}$

The gain becomes

$$G_{11} = \frac{4R_g R_L}{(R_{T1} - R)^2} \qquad (39)$$

where $$-R = \frac{-\omega_1 \omega_2 L_o^2 \gamma^2}{R_{T2}}$$

$$R_{T1} = \mathrm{Re}\,(Z_{11}) + R_{s1} = R_L + R_g + R_1 + R_{s1} .$$

To calculate the bandwidth of the amplifier, using the same notation as in the lower sideband converter, Equation (38) can be rewritten as:

$$G_{11} = \frac{4 R_g R_L}{\left| R_{T1}(1 + j2\delta Q_{T1}) - \frac{R}{(1 + j2\delta Q_{T2}\, \Omega_1/\Omega_2} \right|^2}$$

$$= \frac{4 R_g R_L}{(R_{T1} - R)^2 + 4\delta^2 (R_{T1}Q_{T1} + RQ_{T2}\, \Omega_1/\Omega_2)^2} \qquad (40)$$

For 3 db fractional bandwidth, set denominator of Equation (40) equal to twice that of Equation (39), or

$$2(R_{T1} - R)^2 = (R_{T1} - R)^2 + 4\delta^2 (R_{T1}Q_{T1} + RQ_{T2}\, \Omega_1/\Omega_2)$$

The fractional bandwidth, therefore, can be expressed as:

$$2\delta = \frac{R_{T1} - R}{R_{T1}Q_{T1} + RQ_{T2}\, \Omega_1/\Omega_2} \qquad (41)$$

The gain bandwidth product is defined as

$$(\text{power gain})^{\frac{1}{2}} \quad (\text{fractional bandwidth})$$

$$= \frac{2(R_g R_L)^{\frac{1}{2}}}{R_{T1}Q_{T1} + RQ_{T2}\, \Omega_1/\Omega_2} \cong 2\frac{\Omega_2}{\Omega_1} \quad \frac{1}{Q_{T2}} \quad \left(\frac{R_g R_L}{R^2}\right)^{\frac{1}{2}} \qquad (42)$$

The assumptions and arguments used in calculation of noise figure of the lower sideband converter also apply here. In analogy to Equation (24), if a voltage source E_2 of frequency ω_2 is applied in ω_2 circuit, the power output at frequency ω_1 in the ω_1 circuit can be expressed as:

$$P_{12} = \frac{\frac{R_L}{R_{s2}^2} Q_1^2 E_2^2}{\left|(1 + \frac{Z_{11}}{R_{s1}})(1 + \frac{Z_{22}^*}{R_{s2}}) - Q_1 Q_2\right|^2} \tag{43}$$

The noise voltage in ω_2 circuit is given by:

$$e_{n2}^2 = 4kB\ (T_2 R_2 + T_s R_{s2}) \tag{44}$$

and the noise voltage in ω_1 circuit is given by:

$$e_{n1}^2 = 4kB\ (T_1 R_1 + T_s R_{s1} + T_g R_g) \tag{45}$$

The noise output due to the noise voltage in ω_2 circuit is:

$$N_{12} = \frac{Q_1^2 \frac{R_L}{R_{s2}^2}\ 4kB\ (T_2 R_2 + T_s R_{s2})}{\left|1 + \frac{Z_{11}}{R_{s1}})(1 + \frac{Z_{22}^*}{R_{s2}}) - Q_1 Q_2\right|^2} \tag{46}$$

and from Equation (37), the noise output due to the noise voltage in ω_1, circuit is:

$$N_{11} = \frac{4kB\ (T_1 R_1 + T_s R_{s1} + T_g R_g)\ (\frac{R_L}{R_{s1}^2})\left|1 + \frac{Z_{22}^*}{R_{s2}}\right|^2}{\left|(1 + \frac{Z_{11}}{R_{s1}})(1 + \frac{Z_{22}^*}{R_{s2}}) - Q_1 Q_2\right|^2} \tag{47}$$

The noise factor of the amplifier is therefore:

$$F_1 = \frac{N_{11} + N_{12}}{G_{11} k T_g B}$$

$$= 1 + \frac{T_1 R_1 + T_s R_{s1}}{T_g R_g} + \frac{T_2 R_2 + T_s R_{s2}}{T_g R_g} \frac{Q_1^2}{\frac{(1 + Z_{22}^*)^2}{R_{s2}}} \left(\frac{R_{s1}}{R_{s2}}\right)^2 \qquad (48)$$

At resonance $R_{s2} + Z_{22}^* = R_{s2} + R_2 = R_{T2}$

The noise factor can be expressed as

$$F_1 = 1 + \frac{T_1 R_1 + T_s R_{s1}}{T_g R_g} + \frac{T_s R_s + T_s R_{s2}}{T_g R_g} \left(\frac{R}{R_{T2}}\right) \left(\frac{\omega_1}{\omega_2}\right) \qquad (49)$$

where $R_{T2} = R_{s2} + R_2$

$$- R = \frac{\omega_1 \omega_2 L_o^2 \gamma^2}{R_{T2}}$$

E. Minimum Noise Figures of Parametric Amplifiers

Parametric amplifiers as mentioned earlier can be low-noise devices. One is interested in knowing how low the noise figure can be. We may express the minimum noise figures as a function of the ratio of the signal frequency and the idler frequency, the product of two dynamic quality factors of the parametric element at the signal frequency and the idler frequency, and the ratio of the temperature of the parametric element and the signal generator.

To begin with, the parametric amplifiers are assumed to be operating

in high gain situation, i.e. from Equations (26) and (38):

$$(1 + \frac{Z_{22}}{R_{s2}})(1 + \frac{Z_{11}^*}{R_{s1}}) = (1 + \frac{Z_{22}^*}{R_{s2}})(1 + \frac{Z_{11}}{R_{s1}}) = Q_1 Q_2 \qquad (50)$$

This relation can be rewritten as:

$$\frac{\left| 1 + \frac{Z_{11}^*}{R_{s1}} \right|^2}{Q_2^2} = \frac{Q_1^2}{(1 + \frac{Z_{22}}{R_{s2}})^2} \qquad (51)$$

and

$$\frac{Q_1^2}{(1 + \frac{Z_{22}^*}{R_{s2}})^2} = \frac{(1 + Z_{11}/R_{s1})^2}{Q_2^2} \qquad (52)$$

For the case of a high gain, both ω_1 circuit and ω_2 circuit can be assumed to be at resonance. Therefore, for the lower sideband converter with the input at ω_1 and the output at ω_2 one obtains:

$$Z_{11}^* = R_g + R_1 \qquad Z_{22} = R_2 + R_L \qquad (53)$$

and for the amplifier (input and output at same frequency)

$$Z_{11} = R_g + R_1 + R_L \qquad Z_{22}^* = R_2 \qquad (54)$$

Substituting Equation (53) into Equation (51) for the lower sideband converter, one finds:

$$\frac{(1 + \frac{Z_{11}^*}{R_{s1}})^2}{Q_2^2} = \frac{R_{s1} + R_1 + R_g}{R_{s2} + R_2 + R_L} (\frac{\omega_1}{\omega_2}) (\frac{R_{s2}}{R_{s1}})^2 \qquad (55)$$

Accordingly, Equation (35) can be rewritten:

$$F_2 = 1 + \frac{T_1 R_1 + T_s R_{s1}}{T_g R_g} + \frac{T_2 R_2 + T_s R_{s2}}{T_g R_g} \frac{R_{s1} + R_1 + R_g}{R_{s2} + R_2 + R_L} \frac{\omega_1}{\omega_2} \quad (56)$$

and substituting Equation (54) into Equation (52), for the amplifier

$$\frac{Q_1^2}{(1 + \frac{Z_{22}^*}{R_{s2}})^2} = \frac{R_{s1} + R_1 + R_g + R_L}{R_{s2} + R_2} (\frac{\omega_1}{\omega_2}) (\frac{R_{s2}}{R_{s1}})^2 . \quad (57)$$

Accordingly, for the amplifier, Equation (48) can be rewritten:

$$F_1 = 1 + \frac{T_1 R_1 + T_s R_{s1}}{T_g R_g} + \frac{T_2 R_2 + T_s R_{s2}}{T_g R_g} \frac{R_{s1} + R_1 + R_g + R_L}{R_{s2} + R_2} (\frac{\omega_1}{\omega_2}) \quad (58)$$

Equations (56) and (58) can be further simplified, if we assume:

$$R_L = R_1 = R_2 = \mathrm{Im}(Z_{11}) = \mathrm{Im}(Z_{22}) = 0.$$

Equation (50) becomes:

$$1 + (\frac{R_g}{R_{s1}}) = Q_1 Q_2 . \quad (59)$$

Substituting Equation (59) into Equations (56) and (58) the same minimum noise figures were obtained for the converter and amplifier:

$$F = 1 + \frac{T_s}{T_g} \frac{1}{Q_1 Q_2 - 1} (1 + \frac{\omega_1}{\omega_2} Q_1 Q_2) \quad (60a)$$

For an ideal parametric element, the loss is usually small and can be neglected, i.e. $R_{s1} = R_{s2} = 0$. Also let R_1, R_2 and R_L be small in

comparison with R_g; then the minimum noise figure for an ideal parametric amplifier can be obtained from Equation (58) by inspection:

$$F = 1 + \frac{T_2}{T_g} \frac{\omega_1}{\omega_2} \tag{60b}$$

V. EXPERIMENTAL INVESTIGATION

A. Thin Film Inductors

The 80-20 Ni-Fe permalloy film about 1 micron in thickness was used in this investigation. The substrate of the film is Be-Cu wire of 5 mils in diameter.

The fabrication of the thin film inductor is shown in Figure 2. The number of 44 A. W. G. wire was wound tightly around the glass tube with an outside diameter of approximately 10 mils. The glass tube is not shown in Figure 2. Three thin film inductors have been investigated. Their dimensions are shown in the following:

	Number of Turns	Length of Coils
A	220	3/4"
B	120	1/2"
C	70	1/4"

To study the static characteristics of the thin film inductors, the inductor was characterized by an R_p, L_p and C in parallel. The effect of self-capacitance was taken into consideration. As a result, there was an apparent increase in L_p, the new value being L_e, where:

$$L_e = \frac{L_p}{1 - \omega^2 L_p C} \tag{61}$$

and

$$R_e = R_p \tag{62}$$

The Q was reduced to Q_e, where

$$Q_e = \frac{R_e}{\omega L_e} = \frac{R_p}{\omega L_p} \left(1 - \omega^2 L_p C \right) \tag{63}$$

The Boonton 250-A RX meter was used to measure the L_e and Q_e.

The equivalent series resistance R_s and inductance L can be calculated, where

$$R_s = R_p / (1 + Q_e^2) \tag{64}$$

$$L = L_e Q_e^2 / (1 + Q_e^2) \tag{65}$$

and $$Q = \omega L / R = Q_e \tag{66}$$

Q_e, ωL_e and R_s for three thin film inductors were plotted in Figures 6, 7 and 8 vs. bias current.

B. Parametric Amplifier and Noise Measurement

The schematic diagram of a parametric amplifier is shown in Figure 9. The thin film inductor was connected in series to two high Q tank circuits with 50 ohms cables about 22 inches in length. C_1 and C_2 were tuned to resonate the circuit at ω_1 and ω_2 simultaneously. By loosely coupling the external signal system to the device, the Q of the two tank circuits can be measured. With no external loading, the Q was found to be approximately 40 at 15 mc/s and approximately 25 at 30 mc/s.

From Equation (48), it is evident that the noise factor of a device depends on the value of input impedance (or resistance). It can be shown that the noise factor of an attenuator is equal to loss ratio of

Figure 6. The static characteristics of the thin film inductor A. The subscripts 1 and 2 refer to the values at 30 mc/s and 15 mc/s, respectively.

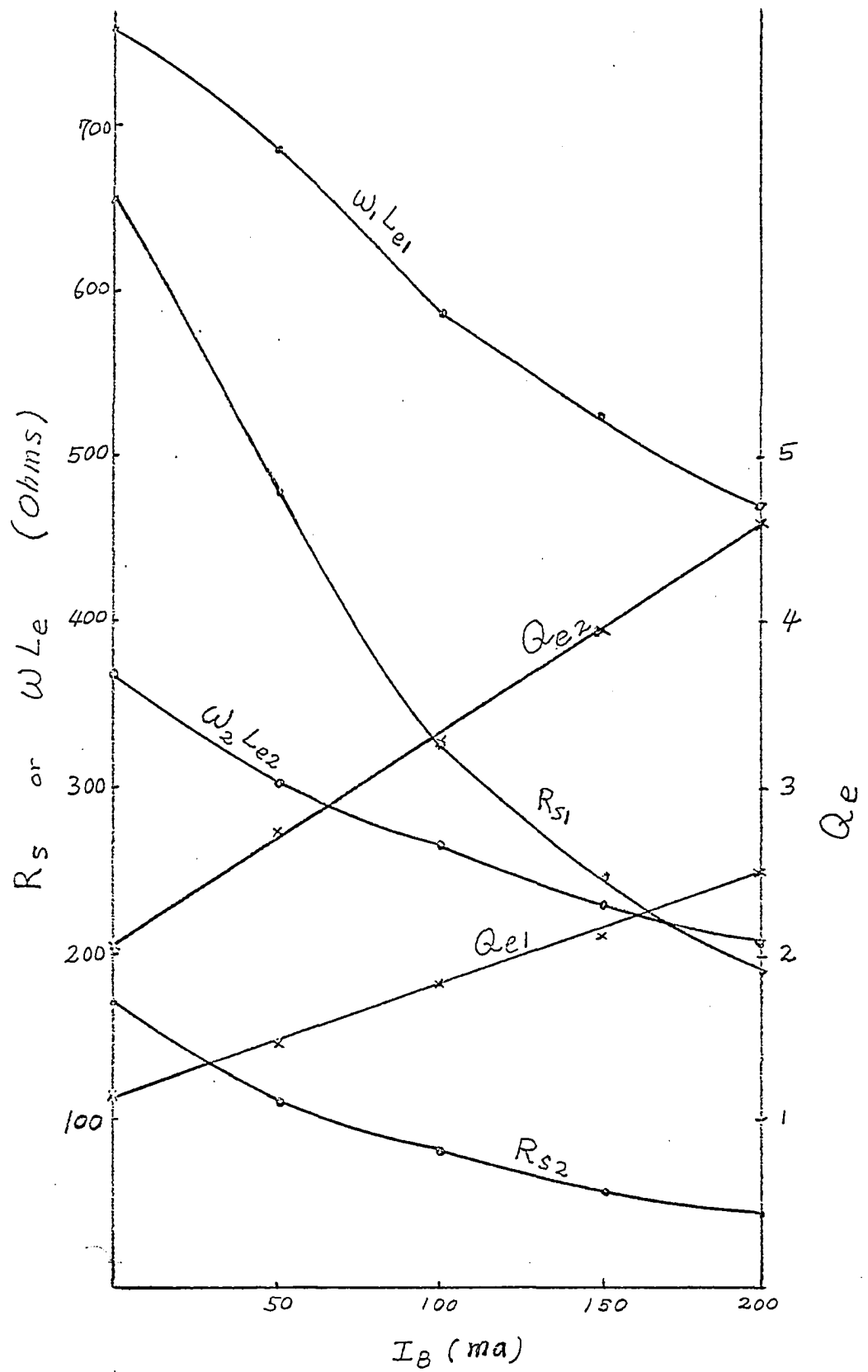
700
600
500
400
300
200
100
R_S or ωL_e (Ohms)
5
4
3
2
1
Q_e
$\omega_1 L_{e1}$
Q_{e2}
$\omega_2 L_{e2}$
R_{S1}
Q_{e1}
R_{S2}
50
100
150
200
I_B (ma)

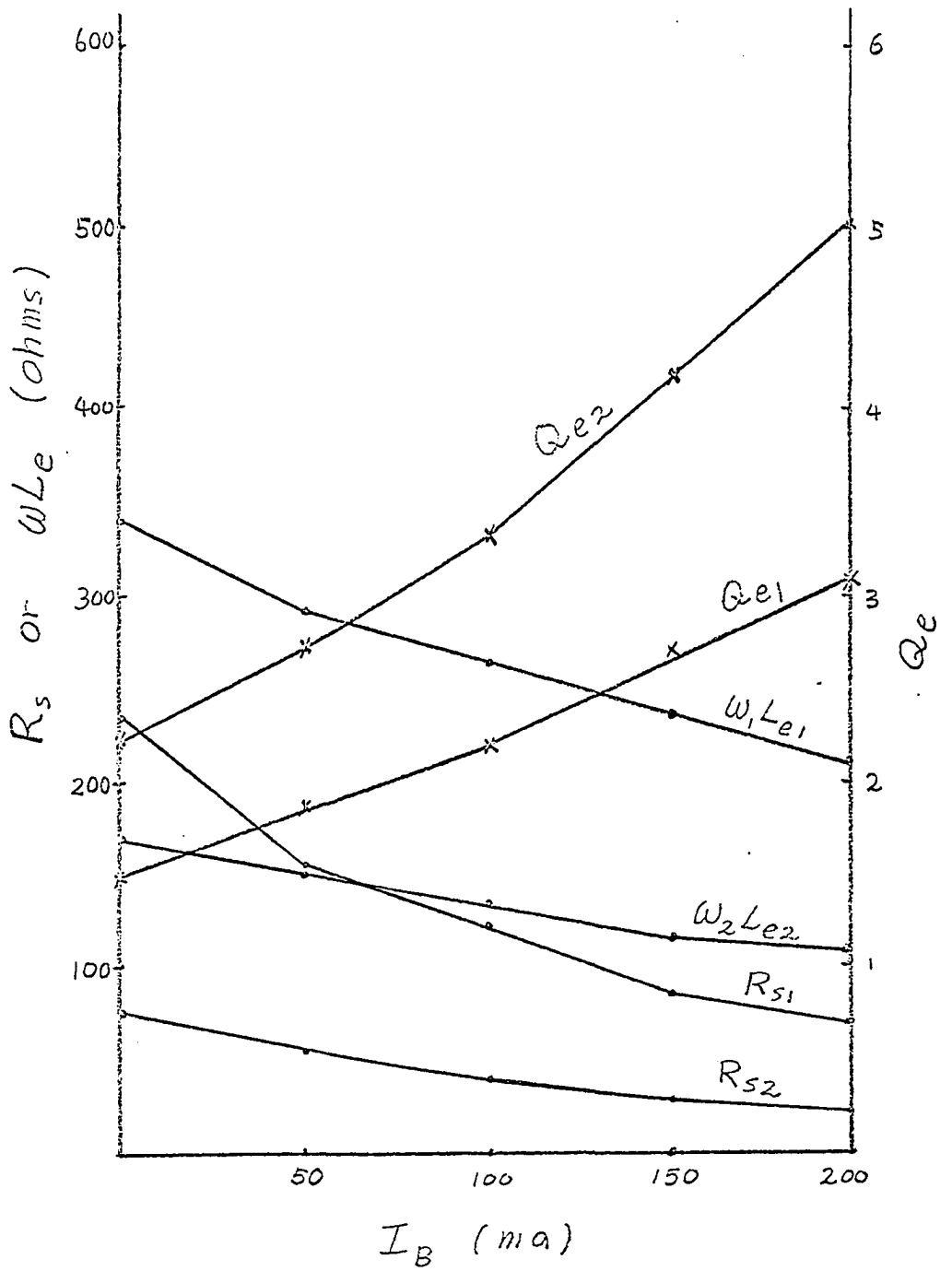

Figure 7. The static characteristics of the thin film inductor B. The subscripts 1 and 2 refer to the values at 30 mc/s and 15 mc/s respectively

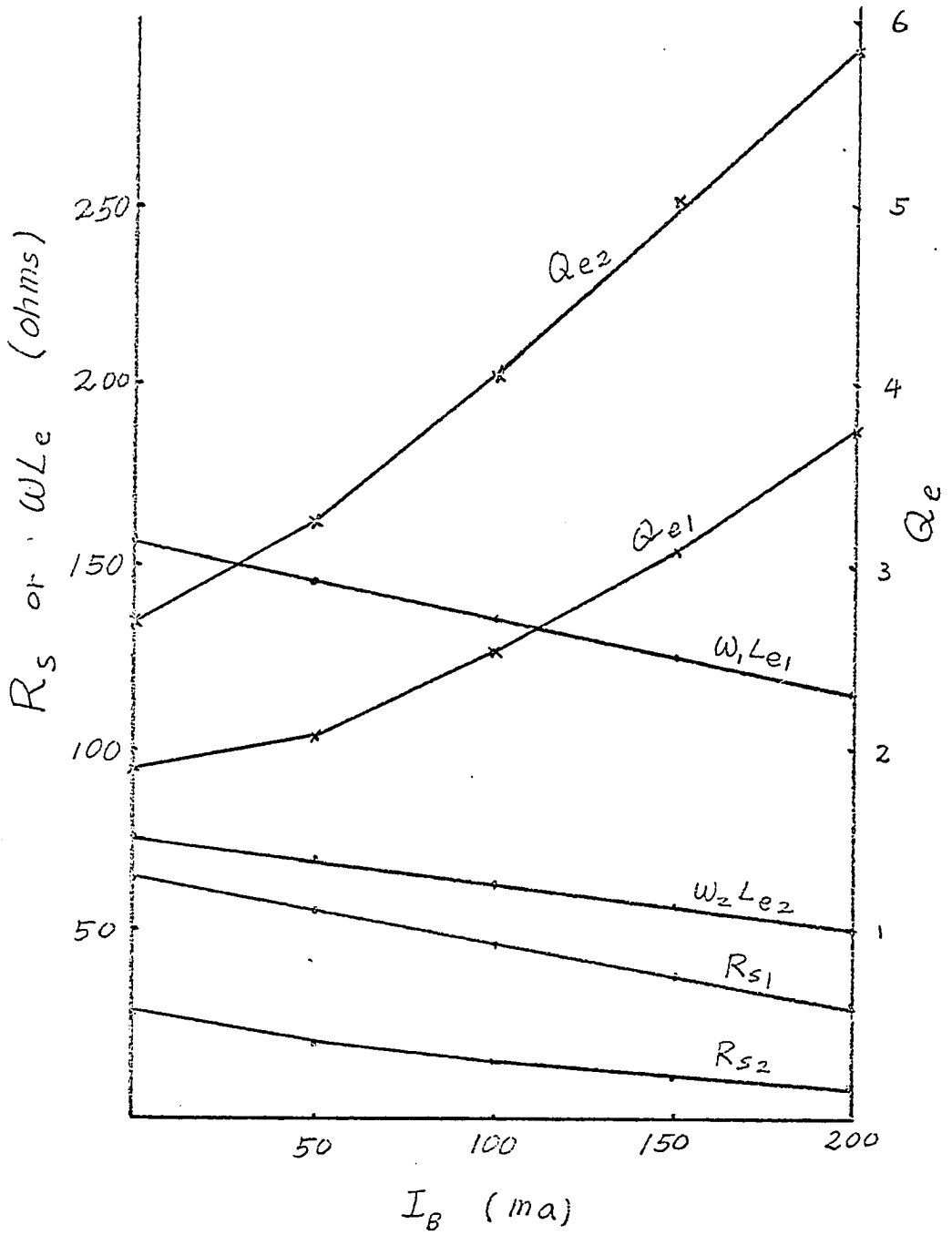

Figure 8. The static characteristics of the thin film inductor C. The subscripts 1 and 2 refer to the values at 30 mc/s and 15 mc/s respectively

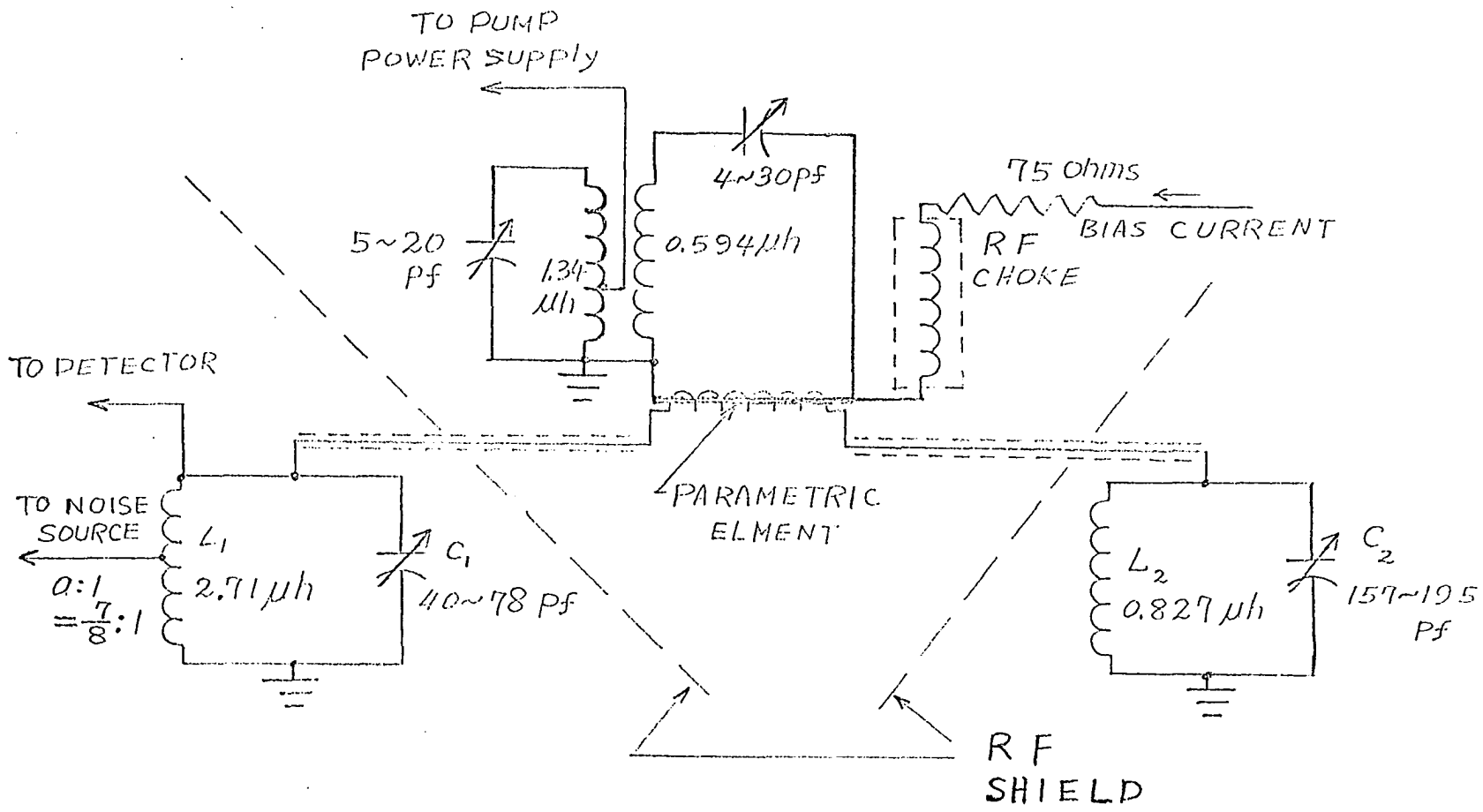

Figure 9. The schematic diagram of the thin magnetic film parametric amplifier for noise measurement

the attenuator (20). Therefore the output was tightly coupled to input to reduce the insertion loss. The insertion loss varied from 0.3 db to 0.9 db depending on the impedance matching and the film loss. Equation (42) indicates that the gain bandwidth product should be constant. Because of the tight coupling to the device, the Q of the system is about 2 and the bandwidth is in the order of 10 mc/s. This limited the noise measurements to relatively low gain operating conditions.

A typical noise measuring system as shown in Figure 10 was used to measure the total noise figure of the system by the twice power method (Appendix).

When two networks of the noise factor F_1 and F_2 and with the available gain G_1 and G_2 are cascaded together, the total noise output is equal to the sum of the noise developed by each separately: hence

$$(F_{12} - 1)k\ To\ B\ G_1G_2 = (F_1 - 1)k\ To\ B\ G_1G_2 + (F_2 - 1)k\ To\ B\ G_2$$

or

$$F_{12} = F_1 + \frac{F_2 - 1}{G_1} \tag{67}$$

where F_{12} is the total noise factor. If F_2 is the noise factor of the power amplifier and the detector, and F_1 and G_1 are the noise factor and the gain of parametric amplifier respectively, F_{12}, F_2 and G_1 can be measured separately. Accordingly F_1 can be calculated from the above equation.

The noise figures (or noise factors) for the experimental parametric amplifiers have been plotted with the pumping voltage and the d.c. bias current as parameters as shown in Figure 11 through Figure 19.

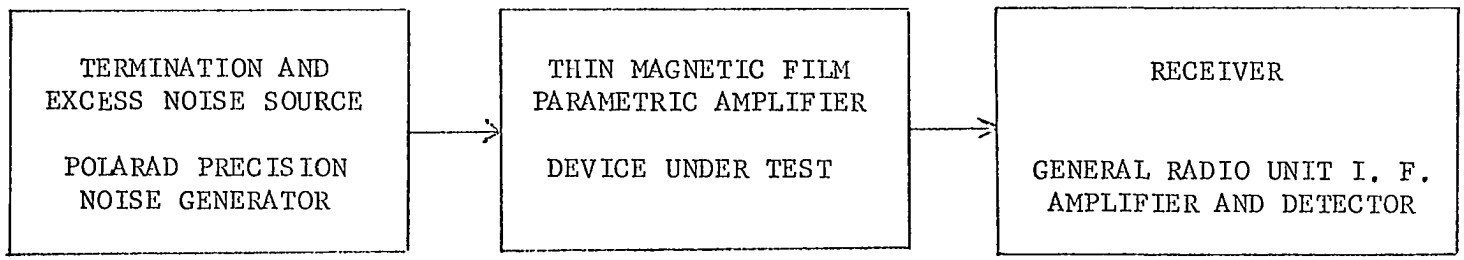

Figure 10. The system and equipments used for noise measurement

Figure 11. Measured noise figures of the thin film parametric amplifier using thin film inductor A with respect to different bias currents at room temperature

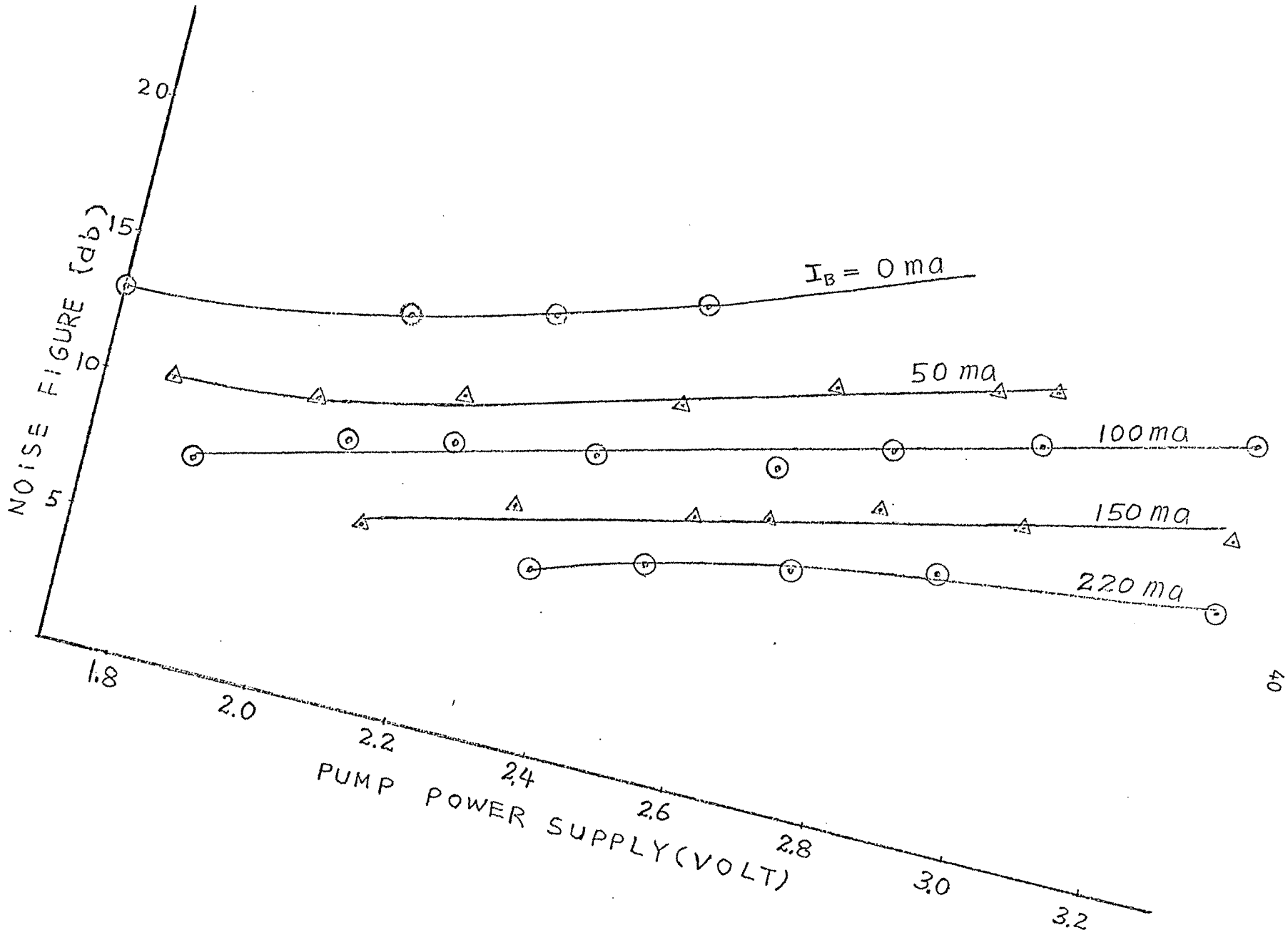
NOISE FIGURE (db)
20
15
10
5
I_B = 0 ma
50 ma
100 ma
150 ma
220 ma
1.8
2.0
2.2
2.4
2.6
2.8
3.0
3.2
PUMP POWER SUPPLY(VOLT)

Figure 12. Measured noise figures of the thin film parametric amplifiers using thin film inductor A with respect to different bias currents when film is cooled to about liquid nitrogen temperature

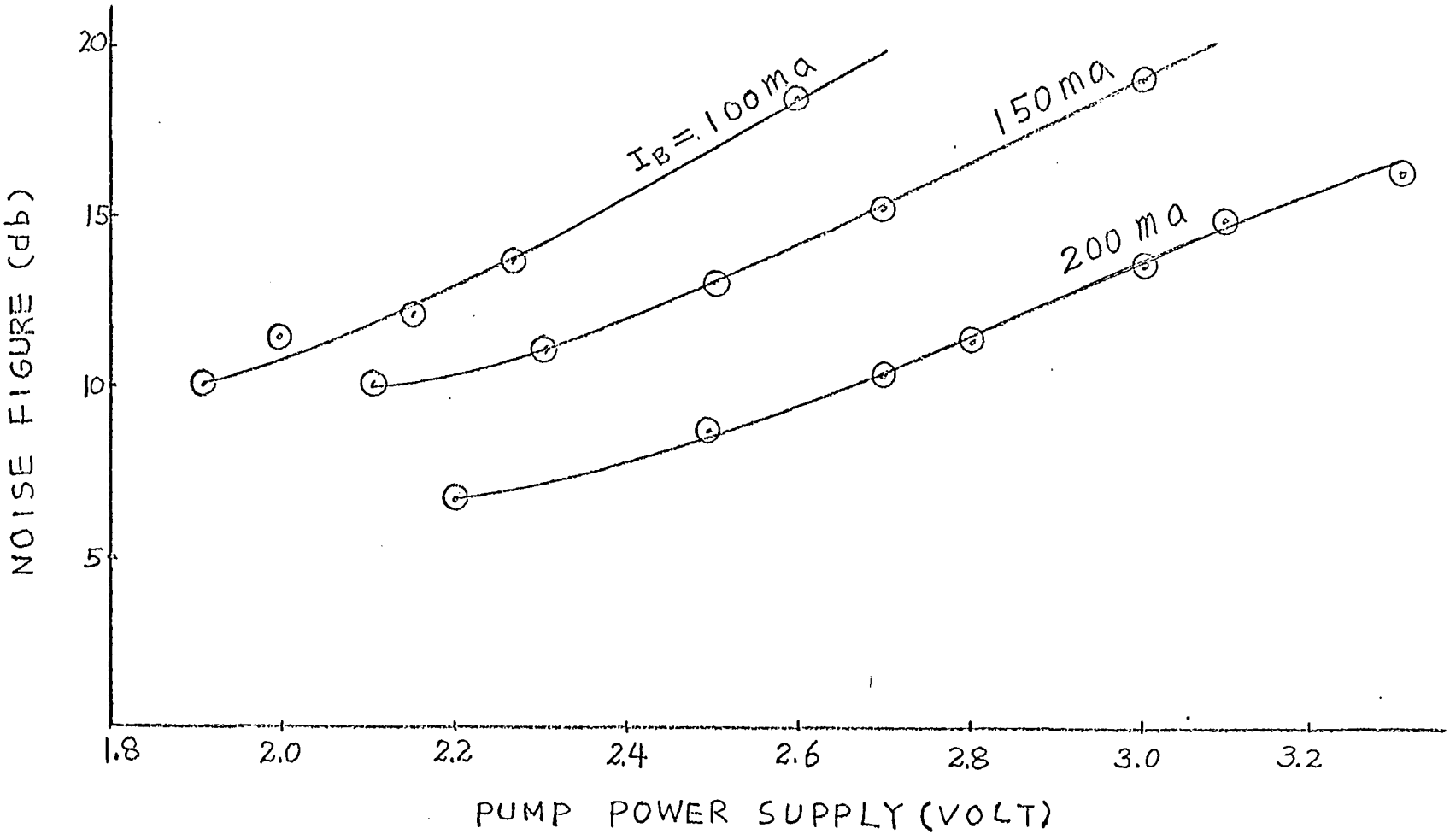
NOISE FIGURE (db)
20
15
10
5
I_B = 100 ma
150 ma
200 ma
1.8
2.0
2.2
2.4
2.6
2.8
3.0
3.2
PUMP POWER SUPPLY (VOLT)

Figure 13. Measured noise figures of the thin film parametric amplifier using thin film inductor B with respect to different bias currents at room temperature

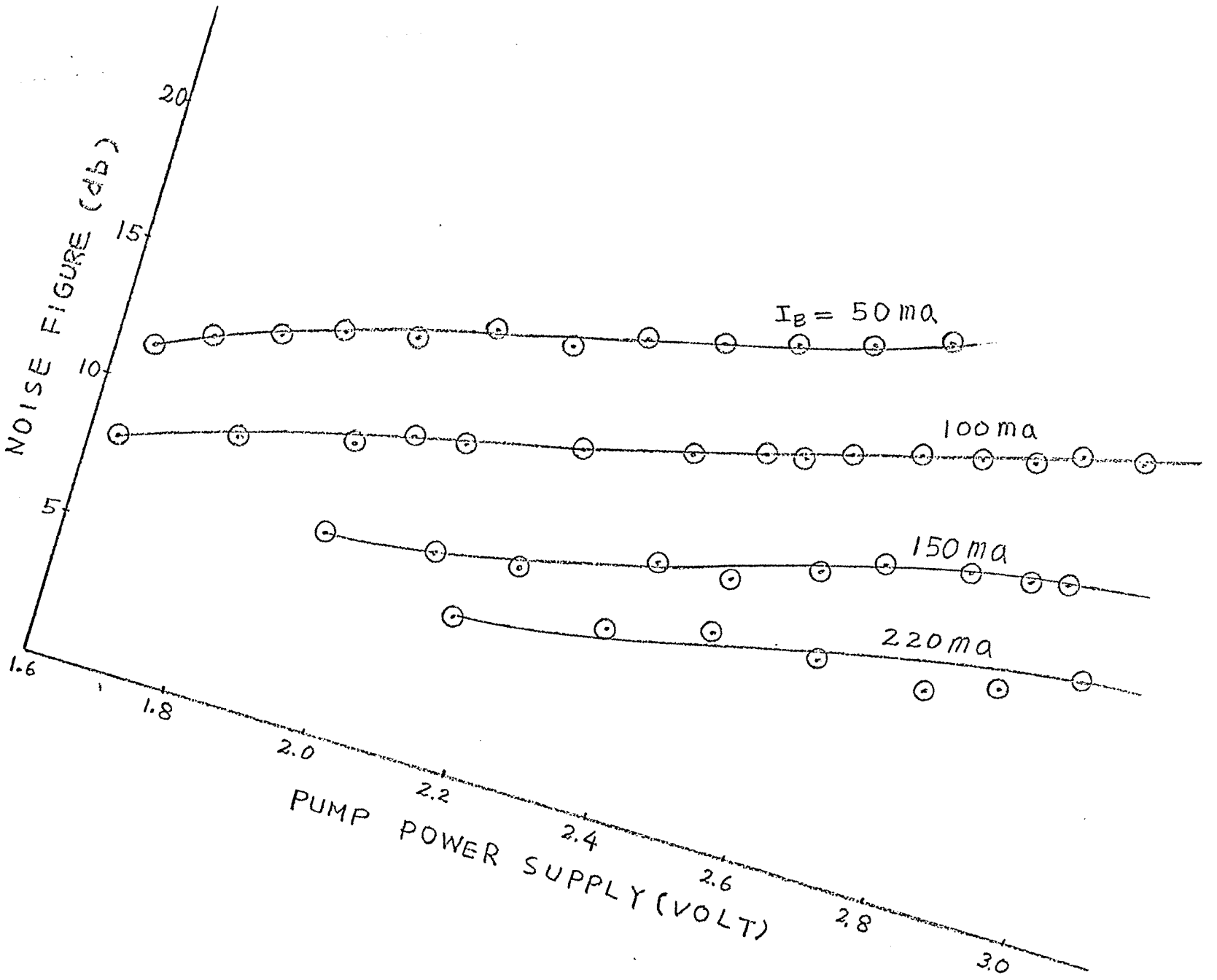
NOISE FIGURE (db)
20
15
10
5
1.6
1.8
2.0
2.2
2.4
2.6
2.8
3.0
PUMP POWER SUPPLY (VOLT)
I_B = 50 ma
100 ma
150 ma
220 ma

Figure 14. Measured noise figures of the thin film parametric amplifier using thin film inductor B with respect to different bias currents when film is immersed into liquid nitrogen

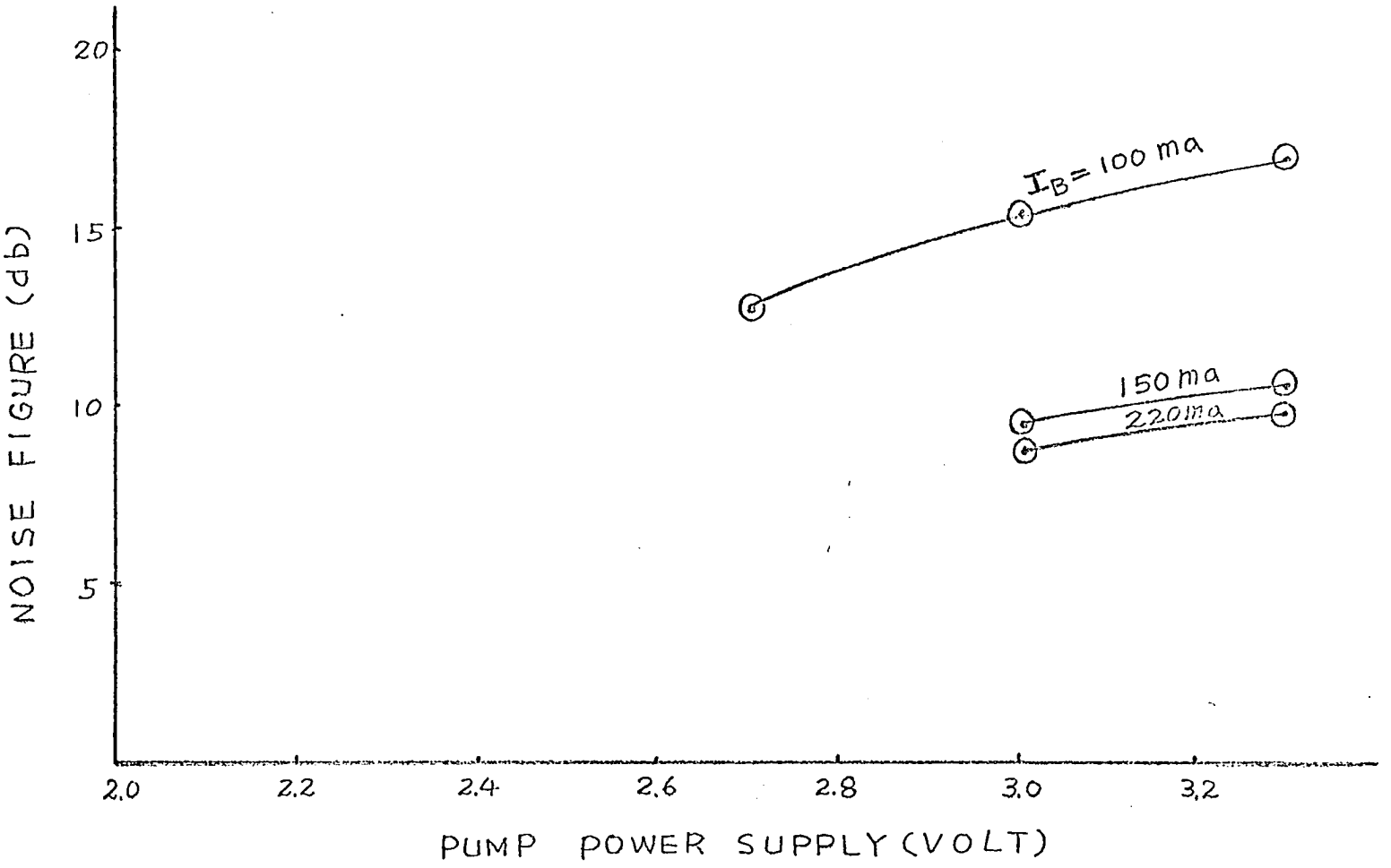
20
15
10
5
NOISE FIGURE (db)
I_B= 100 ma
150 ma
220 ma
2.0
2.2
2.4
2.6
2.8
3.0
3.2
PUMP POWER SUPPLY (VOLT)

Figure 15. Measured noise figures of thin film parametric amplifier using thin film inductor B when film is cooled to about liquid nitrogen temperature

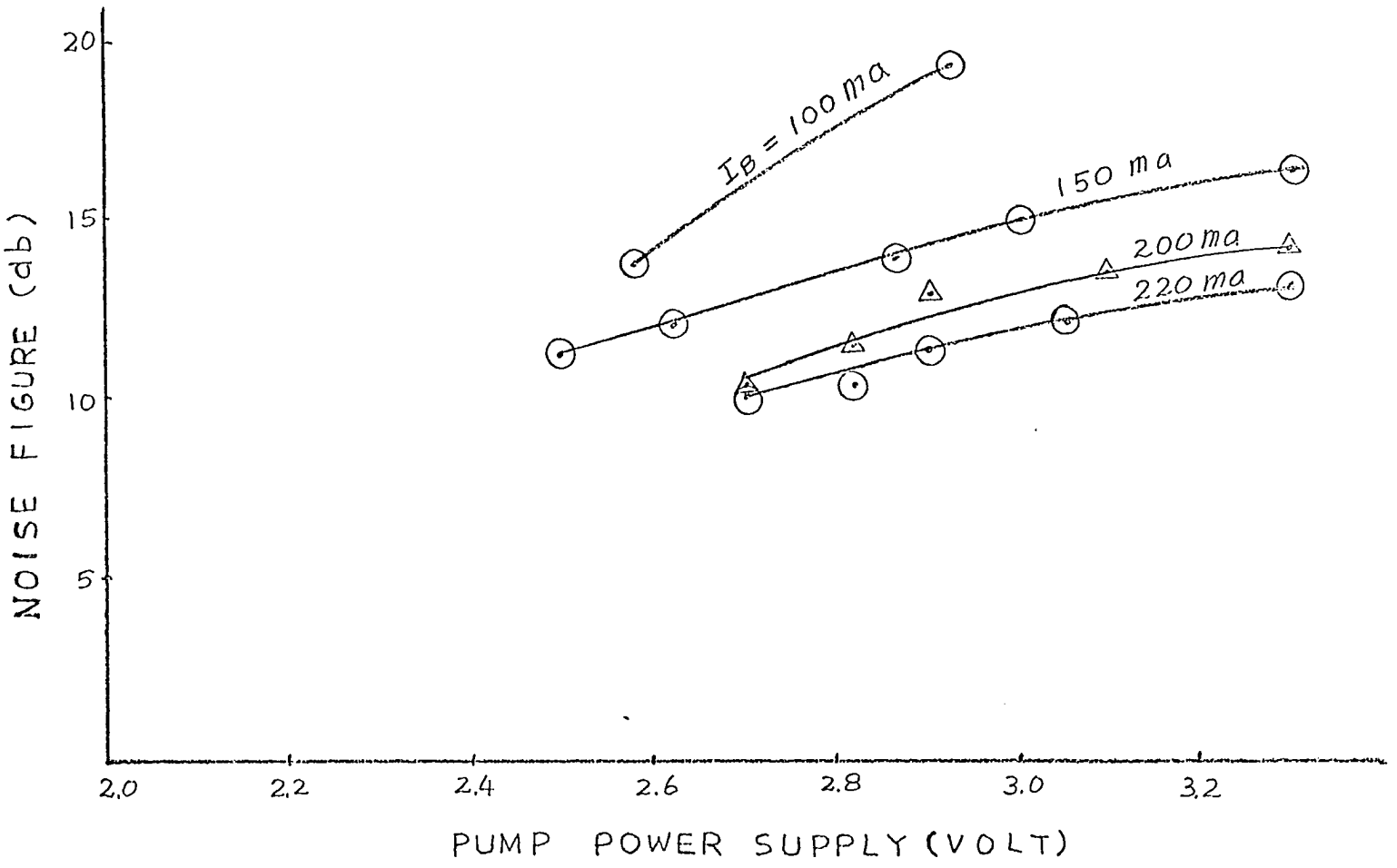
NOISE FIGURE (db)
20
15
10
5
2.0
2.2
2.4
2.6
2.8
3.0
3.2
PUMP POWER SUPPLY (VOLT)
IB = 100 ma
150 ma
200 ma
220 ma

Figure 16. Measured noise figures of the thin film parametric amplifier using thin film inductor C with respect to different bias current at room temperature

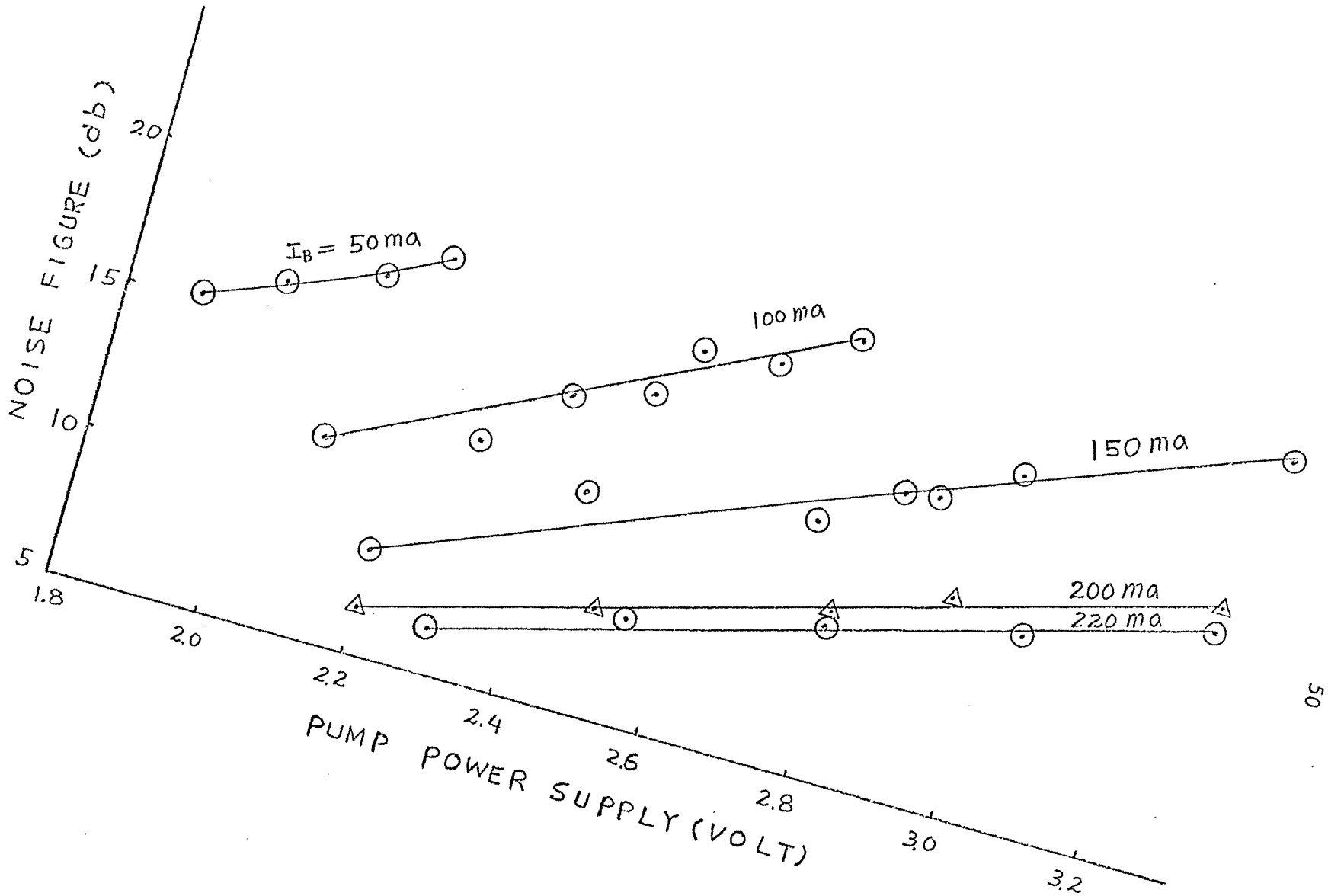
NOISE FIGURE (db)
20
15
10
5
I_B = 50 ma
100 ma
150 ma
200 ma
220 ma
1.8
2.0
2.2
2.4
2.6
2.8
3.0
3.2
PUMP POWER SUPPLY (VOLT)

50

Figure 17. Measured noise figures of the thin film parametric amplifier using thin film inductor C with respect to different bias currents when film is immersed into liquid nitrogen

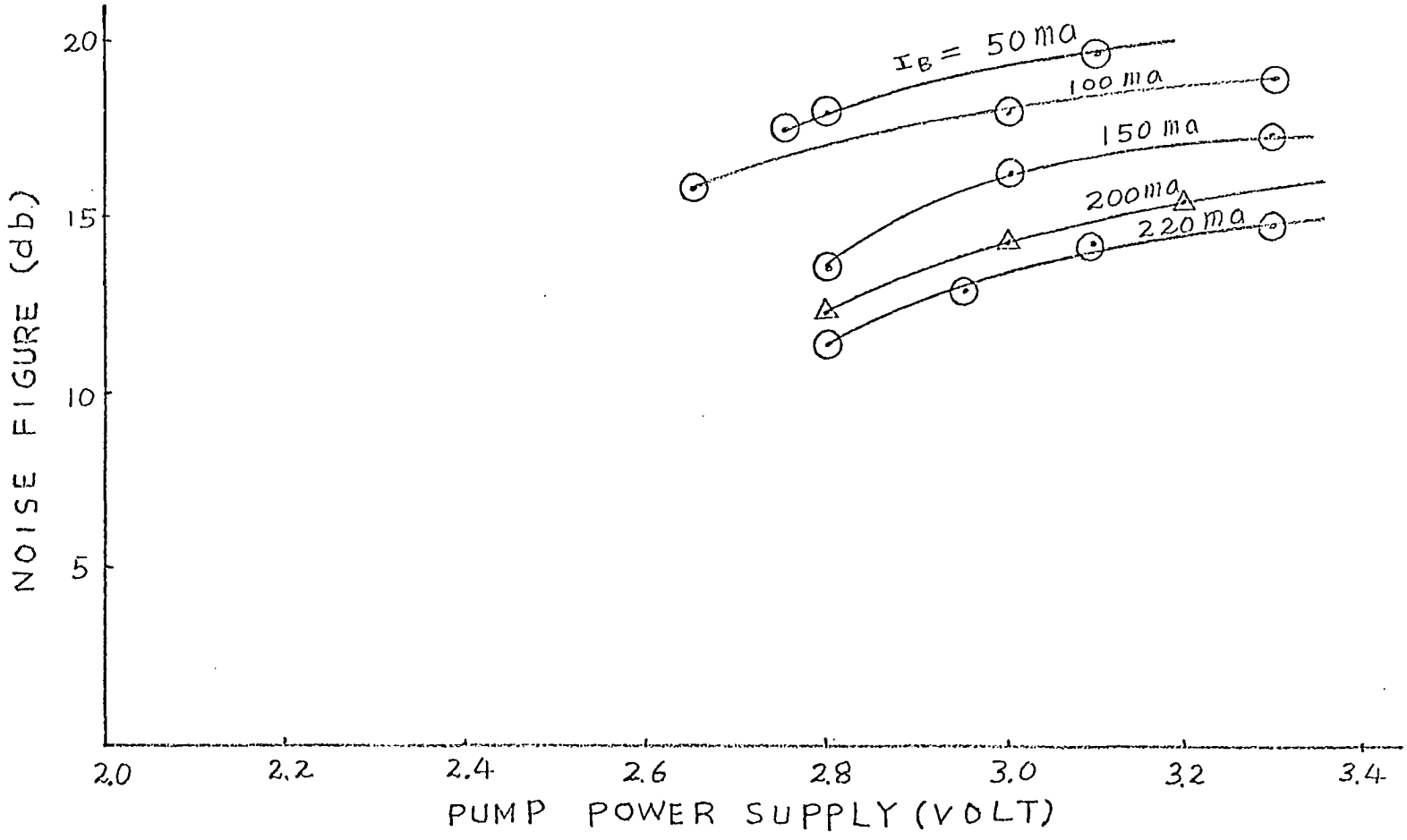
NOISE FIGURE (db.)
20
15
10
5
I_B = 50 ma
100 ma
150 ma
200 ma
220 ma
2.0
2.2
2.4
2.6
2.8
3.0
3.2
3.4
PUMP POWER SUPPLY (VOLT)

Figure 18. Measured noise figures of the thin film parametric amplifier using thin film inductor B with different bias currents at room temperature. Abscissa is calibrated to 274 ma (rms)/volts

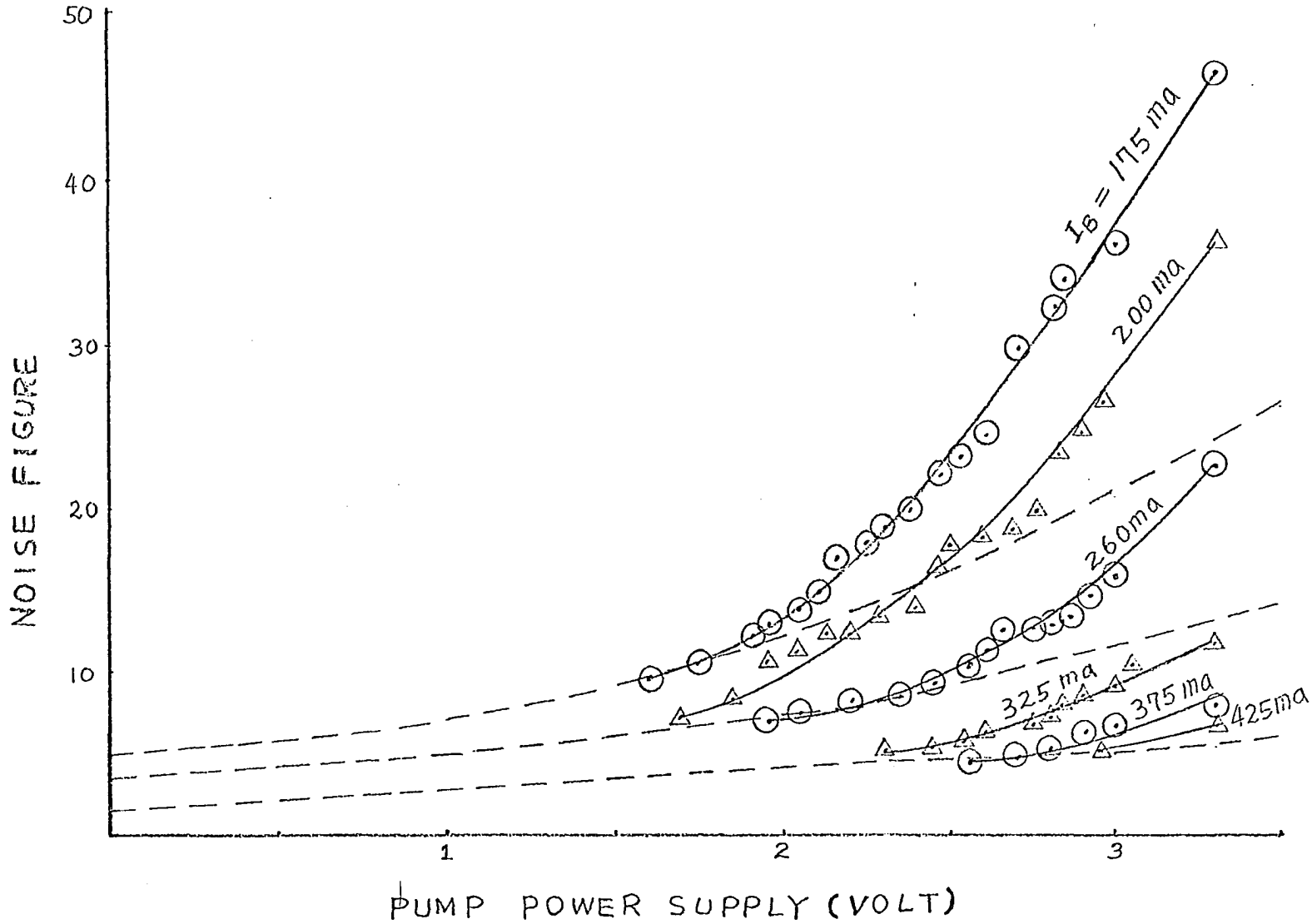
50
40
30
20
10
NOISE FIGURE
1
2
3
PUMP POWER SUPPLY (VOLT)
I_B = 175 ma
200 ma
260ma
325 ma
375 ma
425ma

Figure 19. Measured noise figures of the thin film parametric amplifier using thin film inductor B but with a different film at room temperature

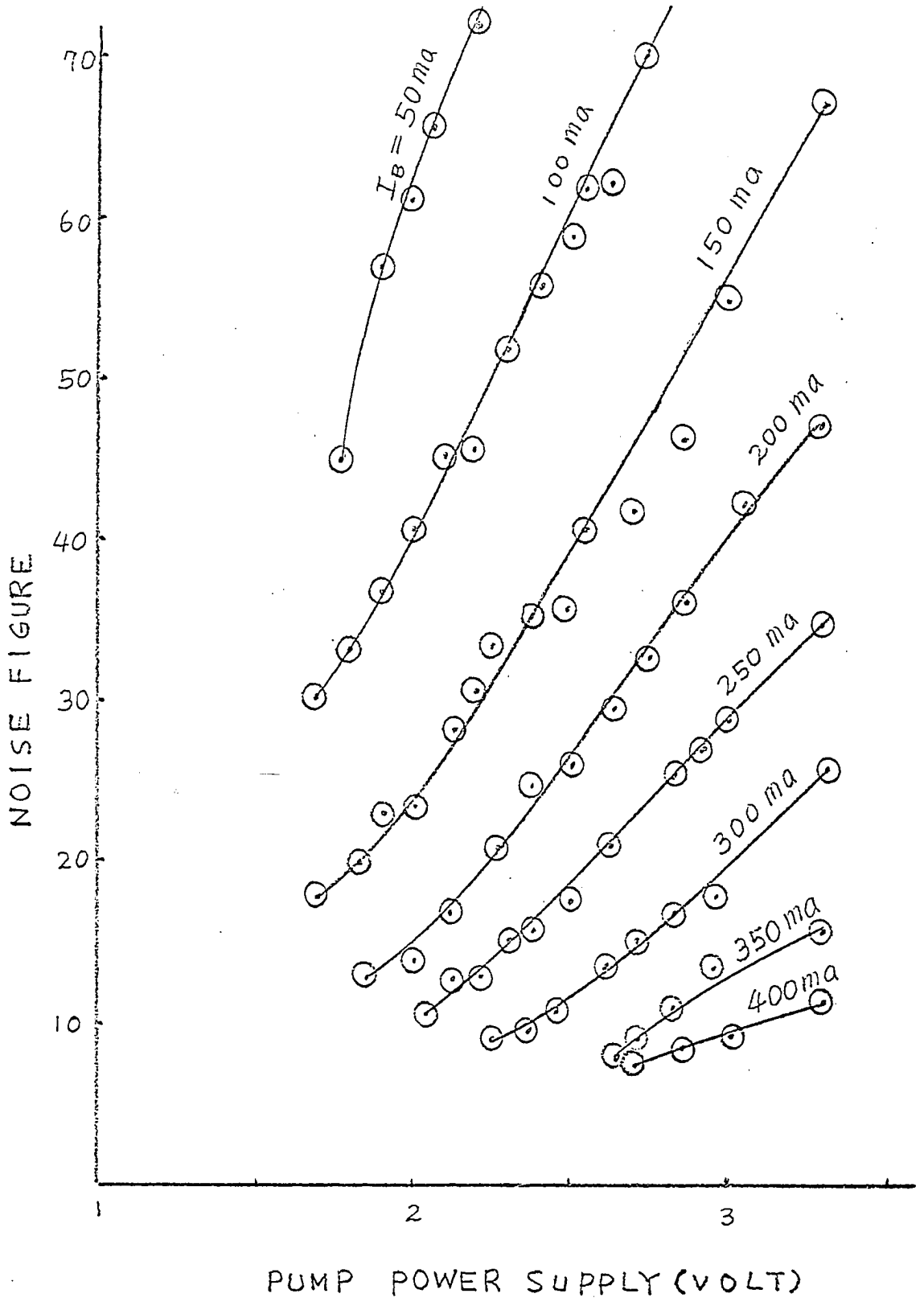
NOISE FIGURE
70
60
50
40
30
20
10
1
2
3
PUMP POWER SUPPLY (VOLT)
I_B = 50 ma
100 ma
150 ma
200 ma
250 ma
300 ma
350 ma
400 ma

At the room temperature, assuming $T_s = T_g$, R_1 and R_2 are small compared with R_{s1}, R_g and R_{s2}, then from Equation (49):

$$F_1 = 1 + \frac{R_{s1}}{R_g} + \frac{R}{R_g}\frac{\omega_1}{\omega_2}$$

$$= 1 + \frac{R_{s1}}{R_g} + \frac{\omega_1^2 L_o^2}{R_{s2} R_g}\gamma^2 \qquad (68)$$

where $\gamma = qVp$, q can be assumed as a constant. If we define:

$$a = 1 + \frac{R_{s1}}{R_g}$$

$$b = (\omega_1^2 L_o^2 / R_{s2} R_g) q^2$$

then the shape of noise factor in terms of pump voltage is:

$$F_1 - a = bV_p^2 \qquad (69)$$

This equation characterizes the noise figures of experimental thin magnetic film parametric amplifiers. To compare the experimental noise figure measurements with the theoretical values, three points at lower pump voltages corresponding to bias currents of 175 ma, 260 ma and 375 ma were used to determine the constants a and b. The three dotted lines on Figure 18 are calculated noise factors vs. pumping voltages. Their equations are:

$F_1 - 4.01 = 2.22\ V_p^2$ for bias current of 175 ma

$F_1 - 3.55 = 0.829\ V_p^2$ for bias current of 260 ma

$F_1 - 1.27 = 0.483\ V_p^2$ for bias current of 375 ma

If the applied pumping field is continuously increased, its magnitude eventually exceeds the sum of the bias field and the coercive force.

Domain walls may appear and Barkhausen noise can occur.

The theoretical minimum noise figure of the experimental parametric amplifier evaluated from Equation (60b) is 3 (or 4.77 db), assuming no loss in the parametric element. The measured minimum noise figures for three different thin film inductors are about 5 (or 7 db). This noise figure corresponds to a relatively high bias current and a lower pumping field. The discrepancy between the calculated noise figure and the measured one primary comes from the thermal noise contributed from the loss of the thin film inductor, (the noise equivalent from the insertion loss).

When the parametric element of a parametric amplifier is cooled to temperature T_s, the noise factor of a parametric amplifier theoretically becomes:

$$F_1 = 1 + \frac{T_s}{T_g}\left(\frac{R_{s1}}{R_g} + \frac{R}{R_g}\frac{\omega_1}{\omega_2}\right) \tag{70}$$

However this result has not been verified experimentally.

It has been observed that at room temperature, the minimum pumping field that is required to overcome the insertion loss increases, in general, with increasing the bias. When the parametric element was cooled to about $78^{\circ}K$ the minimum pumping field decreased and then increased with increasing bias.

C. The Lower Sideband Converter

With an input signal at 15 mc/s applied across the 15 mc/s tank circuit and the output extracted from 30 mc/s tank circuit, a linear amplification of 6 db gain with 0.4 mc/s bandwith was observed for inputs

ranging from -80 dbm to -10 dbm. The amplification of the device was saturated when the input signal was above -10 dbm. The circuit diagram is similar to Figure 9, the difference is that the output signal is extracted from the idler tank circuit. The purpose of developing the lower sideband converter was to observe the output signal as well as the input and pump signal with the oscilloscope. Its minimum noise figure is theoretically the same as the negative resistance parametric amplifier, therefore its noise performance was not experimentally investigated in detail.

VI. DISCUSSION

It is well known that the thermal noise of a parametric amplifier can be reduced by cooling part of circuit elements. For a parametric amplifier with a lossless parametric element, the idler tank circuit can be cooled to improve the noise performance. However, when the loss of a parametric element is higher than that of the idler circuit, the previous analysis shows that the cooling of the parametric element is more effective to improve the noise performance. A number of experiments were performed with the parametric element cooled by the liquid nitrogen. However, the expected improvement in the noise performance at low temperature has not been obtained. The thin film inductor A was cooled at one terminal by the liquid nitrogen from a conductor of length approximately 3 inches, the measured noise figures (Figure 12) was slightly higher than those at room temperature (Figure 11). When the thin film inductors B and C with bias current of 220 ma were immersed in the liquid nitrogen, the measured minimum noise figures with both inductors were 8.96 (Figure 14) and 11.42 db (Figure 17), respectively compared with 5.22 (Figure 13) and 6.71 db (Figure 16) respectively at room temperature. The calculated minimum noise figure of the experimental parametric amplifier is 4.77 db if the loss of the parametric element is neglected.

The hysteresis loop of the magnetic film at various conditions were examined and the results were shown in Figure 20. The magnetic film cooled by liquid nitrogen showed on increase in the anisotropy field and the loss. These indicated that a higher pump field was

Figure 20. The hysteresis curves of the thin film inductor C under cooling or the mechanical stress. The horizontal scale is 2.7 oersted/div.

a) At room temperature without bias current (outer curve), with 100 ma bias current (inner curve) or with 200 ma bias current (inmost curve)

b) The magnetic film was cooled by liquid nitrogen without bias current (outer curve), or with 100 ma bias current (inner curve)

c) The magnetic film was cooled by the liquid nitrogen with 100 ma bias current (outer curve) or with 200 ma bias current (inner curve)

d) The magnetic film was heated with a soldering iron at one terminal and cooled with liquid nitrogen at the other terminal and also with 100 ma bias current

e) The plated wire was twisted by 180 degrees angle and with 100 ma bias current

f) The plated wire was twisted by 180 degrees angle and without bias current

g) The plated wire was twisted by 180 degrees angle and with 200 ma bias current

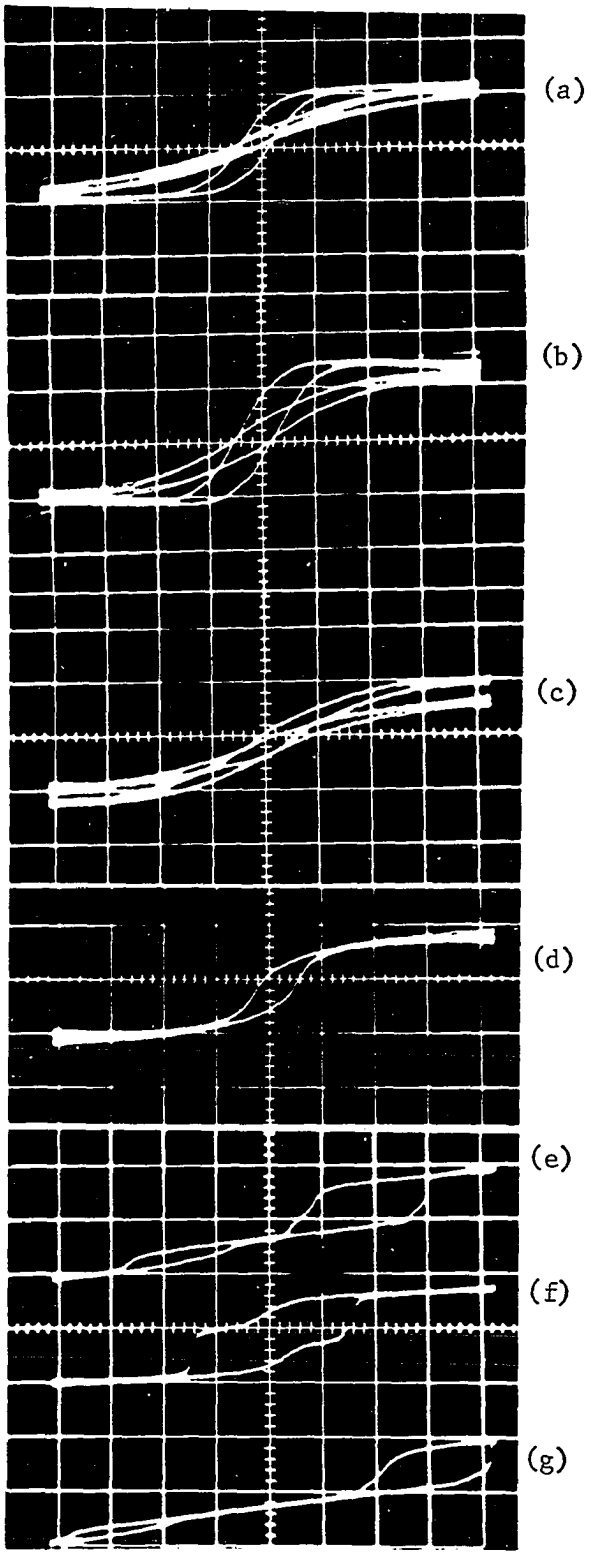
(a)
(b)
(c)
(d)
(e)
(f)
(g)

required in the operation of the thin film parametric amplifier at the low temperature than at room temperature. The increased loss as evidenced by the opening of the 60 cps hysteresis loop was obviously due to domain rearrangement and consequently would add greatly to the Barkhausen noise.

At room temperature the copper resistance of the thin film inductor B at 30 mc/s is 4.13 ohms; the I^2R loss from this resistance is less than 4 per cent of the core loss with 100 ma bias current, or less than 6 per cent of the core loss with 200 ma bias current. At $78^{o}K$ the copper loss will be decreased by about 82 per cent. This indicates that the copper loss of a thin film inductor is small compared with the core loss. Figure 20 (b) and (c) show the strain induced core loss at the low temperature is much higher than that in the room temperature. This demonstrates that the thermal noise contributed from the particular thin film inductor examined cannot be reduced by cooling the parametric element. These experimental results demonstrate that other inductor fabrication techniques must be used to achieve good low temperature performance.

When the thin film inductor is used as a parametric element, the operating field region should keep within the stable field region where the magnetization is conserved. A low noise figure is expected for this type of operation. When the external alternating field exceeds the sum of the bias field and the wall coercive force, the film will start to break up into multidomains, and domains will move by wall motion or rotation to keep the sum of magnetic energies minimum.

The inverse switching time of a permalloy film is known as a function of the longitudinal field as well as the transverse field. When the longitudinal field slightly exceeds the coercive force, the switching time from the data of Olson and Pohm (21) is large (1 μsec or more). In this region the domain moves mainly by the wall motion. The Barkhausen noise caused by this slow wall movement is quite small in our experimental parametric amplifier because the pump field is too fast to allow this slow wall movement. As the longitudinal drive field increases, the switching time decreases. The switching time for uniform or nonumiform rotation is less than 0.1 μsec. This kind of fast flux reversal starts, in the case of a longitudinal drive field only, at about three times the value of H_k (21) (22). Experimentally at room temperature, it is found from Figure 18 that the measured noise figure of 4.69 (6.71 db) where the noise just beginning to increase corresponded to 375 ma bias current and 2.55 volts (rms) pump voltage. For this operating condition the difference between the pump field and the bias field was 10.9 oe which is about four times the value of H_k (approximately 2.5 oe). This experimental result indicated that the magnetization could rotate nearly coherently about its position of equilibrium, even when the pump field exceeded the sum of the bias field and the anisotropy field provided it was not too large. However when the pump field became sufficiently large the partial switching of the film contributed a major portion of the total Barkhausen noise.

For better noise performance and higher gain bandwidth product,

the ratio of the signal frequency to the idler frequency should be low provided the dynamic quality factor of the parametric element can be reasonably high and a good coupling between the thin magnetic film and the coil is achieved. Theoretically the pump frequency can be as high or higher than the resonant frequency of the permalloy film, which is typically about 400 mc/s.

BIBLIOGRAPHY

1. Hartley, R. V. L. Oscillations in system with nonlinear reactance. Bell System Technical Journal 15: 424-440. 1936.

2. Van der Ziel, A. On the mixing properties of nonlinear capacitances. Journal of Applied Physics 19: 999-1006. 1948.

3. Rowe, H. E. Some general properties of non-linear elements. II. Small signal theory. Institute of Radio Engineers Proceedings 46: 850-861. 1958.

4. Manley, J. M. and Rowe, H. E. Some general properties of non-linear elements. Part I. General energy relations. Institute of Radio Engineers Proceedings 44: 904-913. 1956.

5. Uenohara, M. Noise considerations of the variable capacitance parametric amplifier. Institute of Radio Engineers Proceedings 48: 169-179. 1960.

6. Knechtli, R. C. and Weglein, R. D. Low-noise parametric amplifier. Institute of Radio Engineers Proceedings 48: 1218-1226. 1960.

7. Read, A. A. and Pohm, A. V. Magnetic film parametric amplifiers. National Electronics Conference Proceedings 15: 65-78. 1959.

8. Pohm, A. V., Read, A. A., Stewart, R. M., Jr. and Schauer, R. F. High frequency magnetic film parametrons for computer logic. National Electronics Conference Proceedings 15: 202-214. 1959.

9. Samuels, Robert L. Noise characteristics of thin ferromagnetic film devices. Unpublished Ph. D. thesis. Ames, Iowa, Library, Iowa State University of Science and Technology. 1963.

10. Kurokawa, K. and Uenohara, M. Minimum noise figure of the variable-capacitance amplifier. Bell System Technical Journal 40: 695-722. 1961.

11. Rodichev, A. M. and Ignatchenko, V. A. The dynamics of Barkhausen effect. Physics of Metals and Metallography 9; No. 6: 93-98. 1960.

12. Tebble, R. S. and Newhouse, V. L. The Barkhausen effect in single crystals. Physical Society (London) Series B, 66: 633-641.

13. Salanskiy, N. M. and Rodichev, A. M. Length of Barkhausen impulses in ferromagnetics. Physics of Metals and Metallography 17, No. 1, 136-138. 1964.

14. Krumhansl, J. A. and Beyer, R. T. Barkhausen noise and magnetic amplifiers. II. Analysis of the noise. Journal of Applied Physics 20: 582-586. 1949.

15. Biorci, G. and Pescetti, D. Frequency spectrum of the Barkhausen noise. Journal of Applied Physics 28: 777-781. 1957.

16. Stierstadt, K. and Pfrenger, E. Die temperaturabhangigkeit des magnetischen Barkhausen-Effekts. I. Zeitschrift fur Physik 179: 182-198. 1964.

17. Kirenskiy, L. V., Salanskiy, N. M. and Rodichev, A. M. Barkhausen effect where the hysteresis loop is nearly rectangular. Physics of Metals and Metallography 16, No. 4: 130-131. 1963.

18. Landau, L. and Lifshitz, E. The theory of the dispersion of magnetic permeability in ferromagnetic bodies. Physik Zeitschrift der Sowjetunion 8: 153-169. 1935.

19. Pohm, A. V. Switching mechanisms in thin ferromagnetic films. In Prywes, N., ed. Amplifier and memory devices with films and diodes. pp. 225-224. New York, New York, McGraw-Hill Book Co. 1965.

20. Blackwell, L. A. and Kotzebue, K. L. Semiconductor-diode parametric amplifiers. Englewood Cliffs, N. J., Prentice-Hall, Inc. 1961.

21. Olson, C. D. and Pohm, A. V. Flux reversal in thin films at 82% Ni, 18% Fe. Journal of Applied Physics 29: 274-282. 1958.

22. Humphrey, F. B. Flux reversal at low temperatures. Journal of Applied Physics 35: 911-912. 1964.

23. Nyquist, H. Thermal agitation of electric charge in conductors. Physical Review 32: 110-113. 1928.

24. Johnson, J. B. Thermal agitation of electricity in conductors. Physical Review 32: 97-109. 1928.

25. IRE standards on electron tubes: definition of terms, 1957. Institute of Radio Engineers Proceedings 45: 983-1010. 1957.

VIII. ACKNOWLEDGEMENTS

The author wishes to thank his major professor Dr. A. V. Pohm for his guidance, suggestions and encouragement. He also wishes to acknowledge that this investigation was supported by the thin film grant. Thanks also go to Drs. G. E. Fanslow and R. L. Samuels for invaluable discussions in developing the thin magnetic film parametric amplifiers and to Mrs. Sharion McBride for typing the thesis.

IX. APPENDIX

A. Thermal Noise and the Twice-Power Method of Manual Noise Figure Measurement

Thermal Noise (also called Johnson Noise) is the noise caused by thermal agitation in a dissipative body. The available thermal noise power N, from a resistor at temperature T_o, is kT_oB where k is the Boltzmann's constant and B is the frequency interval concerned. This relation was derived by Nyquist (23) in 1928 and experimentally verified by Johnson (24).

The noise performance of the transducer is commonly rated by comparing the noise-power outputs of the actual transducer and of its noise-free equivalent. One such measure of performance is the noise factor (noise figure).

The noise factor (of a two-port transducer) at a specified input frequency is the ratio of (a) the total noise power per unit bandwidth at a corresponding output frequency available at the output port to (b) that portion of (a) engendered at the input frequency by the input termination at the standard noise temperature ($290^{o}k$) (25). If the noise temperature at a pair of terminals can be represented by a resistance at the standard temperature, then the available noise power at the terminal is equal to the available thermal noise power from the resistor. Therefore,

$$\text{Noise factor} = F = \frac{N_o}{G\ kT_oB}$$

where N_o = Available output noise power

G = Available gain of the transducer or the ratio of the available output signal power to the available input signal power (= S_o/S_i).

The noise factor therefore, can be rewritten as

$$F = \frac{(S_i/N_i)}{(S_o/N_o)}$$

where $N_i = kT_oB$ = Available input noise power.

Of the total noise power output of a system ($n_o = kT_oBGF$), we know that a specific portion is the result of amplified input noise (kT_oBG). The amount of noise power added by the receiver (N_r) is:

$$N_r = N_o - kT_oBG$$

$$= (F - 1)\ kT_oBG$$

If a known level of broadband noise can be introduced at the input of a receiver under test, a differential power measurement at the output would indicate a gain bandwidth product of a receiver.

A broadband noise source is usually made of diode or gas discharge tube. Available excess power from the fired noise source then can be expressed as:

$$P = k(T_2 - T_o)\ B$$

where T_2 is the equivalent absolute temperature of the noise source.

Now the excess noise source is connected to input of a receiver with available gain G. The output is measured with a power detector. If we defined

N_1 = total output noise power when theexcess noise source is "cold" or at $290^{o}k$

N_2 = total output noise power when the excess noise source is "fired" or at temperature T_2

Taking the ratio of these measured power we have:

$$\frac{N_2}{N_1} = \frac{\text{(input termination) x G + (receiver) + (excess noise)G}}{\text{(input termination)G + (receiver)}}$$

$$= \frac{kT_oBG + (F - 1)kT_oBG + k(T_2 - T_o)BG}{kT_oBG + (F - 1)kT_oBG}$$

$$= \frac{FT_o + (T_2 - T_o)}{FT_o}$$

and accordingly

$$F = \frac{(T_2 - T_o)}{T_o} \qquad \frac{1}{(\frac{N_2}{N_1} - 1)}$$

In the logarithmic notation

$$F(db) = 10\log F = 10\log (\frac{T_2 - T_o}{T_o}) - 10 \log (\frac{N_2}{N_1} - 1)$$

If we set $N_2 = 2N_1$, then

$$F(db) = 10 \log (\frac{T_2 - T_o}{T_o})$$

and noise factor

$$F = (\frac{T_2 - T_c}{T_o})$$

Therefore the noise figure of the receiver can be measured by directly reading the scale of noise source.